Υπολογισμοί και εφαρμογές της μαγνητικής ελικότητας σε αστροφυσικά περιβάλλοντα

Κώστας Μωραΐτης

LESIA, Observatoire de Paris, CNRS

Outline

- Introduction
  - Magnetic helicity
    - Definition - Properties
  - Applications
  - Relative magnetic helicity
- Numerical computations of relative magnetic helicity
  - Cartesian geometry - Comparison with other methods
  - Spherical geometry
- Relative magnetic field line helicity
  - Definition - Validation
  - Visualization
- Conclusions

Outline

- Introduction
  - Magnetic helicity
    - Definition - Properties
  - Applications
  - Relative magnetic helicity
- Numerical computations of relative magnetic helicity
  - Cartesian geometry - Comparison with other methods
  - Spherical geometry
- Relative magnetic field line helicity
  - Definition - Validation
  - Visualization
- Conclusions

Magnetic helicity

- Signed scalar quantity (right (+), or left (-) handed), defined as $H = \int_V \boldsymbol{A} \cdot \boldsymbol{B} \, dV$ $\boldsymbol{B} = \nabla \times \boldsymbol{A}$

Magnetic helicity

- Signed scalar quantity (right (+), or left (-) handed), defined as $H = \int_V \boldsymbol{A} \cdot \boldsymbol{B} \, dV$ $\boldsymbol{B} = \nabla \times \boldsymbol{A}$
- Units of magnetic flux squared, i.e., Wb^2 in SI, Mx^2 in cgs

Magnetic helicity

- Signed scalar quantity (right (+), or left (-) handed), defined as $H = \int_V \boldsymbol{A} \cdot \boldsymbol{B} \, dV$ $\quad \boldsymbol{B} = \nabla \times \boldsymbol{A}$
- Units of magnetic flux squared, i.e., Wb^2 in SI, Mx^2 in cgs
- Kinetic helicity in fluid dynamics (***B***→vorticity $\boldsymbol{\omega} = \nabla \times \boldsymbol{u}$),
  particle helicity in particle physics (the projection of the spin onto the direction of momentum)

Magnetic helicity

- Signed scalar quantity (right (+), or left (-) handed), defined as $H = \int_V \boldsymbol{A} \cdot \boldsymbol{B} \, dV$ $\boldsymbol{B} = \nabla \times \boldsymbol{A}$
- Units of magnetic flux squared, i.e., Wb^2 in SI, Mx^2 in cgs
- Kinetic helicity in fluid dynamics (***B***→vorticity $\boldsymbol{\omega} = \nabla \times \boldsymbol{u}$),
  particle helicity in particle physics (the projection of the spin onto the direction of momentum)
- It is a geometrical measure of the twist and writhe of the magnetic field lines,
  and of the amount of flux linkages between pairs of lines (Gauss linking number)

Magnetic helicity

- Signed scalar quantity (right (+), or left (-) handed), defined as $H=\int_V \boldsymbol{A}\cdot\boldsymbol{B}\, dV$ $\boldsymbol{B}=\nabla\times\boldsymbol{A}$
- Units of magnetic flux squared, i.e., Wb^2 in SI, Mx^2 in cgs
- Kinetic helicity in fluid dynamics (***B***→vorticity $\boldsymbol{\omega}=\nabla\times\boldsymbol{u}$),
  particle helicity in particle physics (the projection of the spin onto the direction of momentum)
- It is a geometrical measure of the twist and writhe of the magnetic field lines,
  and of the amount of flux linkages between pairs of lines (Gauss linking number)

single flux tube

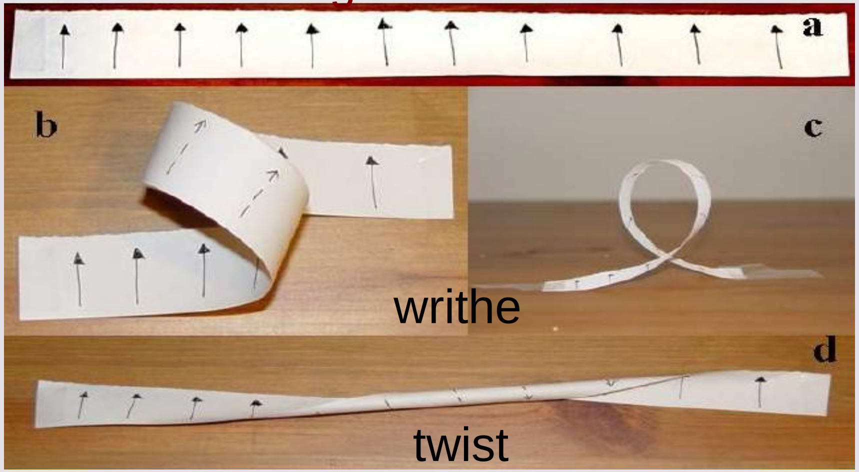

$H=(Tw+Wr)\,\Phi^2$

Magnetic helicity

- Signed scalar quantity (right (+), or left (-) handed), defined as $H = \int_V \boldsymbol{A} \cdot \boldsymbol{B} \, dV$ $\boldsymbol{B} = \nabla \times \boldsymbol{A}$
- Units of magnetic flux squared, i.e., Wb^2 in SI, Mx^2 in cgs
- Kinetic helicity in fluid dynamics (**B**→vorticity $\boldsymbol{\omega} = \nabla \times \boldsymbol{u}$), particle helicity in particle physics (the projection of the spin onto the direction of momentum)
- It is a geometrical measure of the twist and writhe of the magnetic field lines, and of the amount of flux linkages between pairs of lines (Gauss linking number)

single flux tube

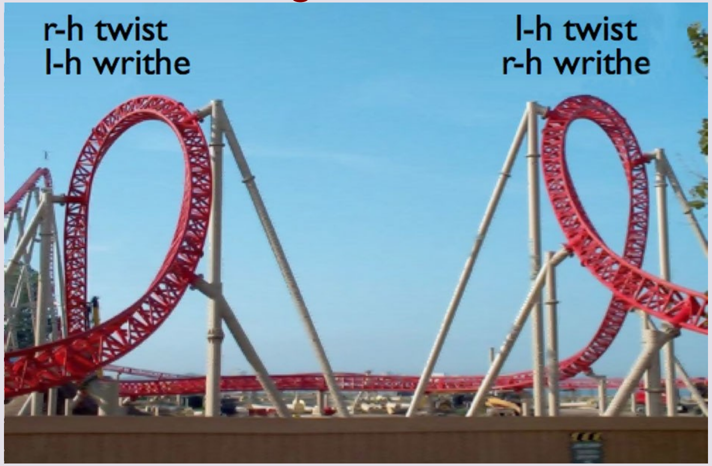

$$H = (Tw + Wr)\,\Phi^2$$

Magnetic helicity

- Signed scalar quantity (right (+), or left (-) handed), defined as $H = \int_V \boldsymbol{A} \cdot \boldsymbol{B} \, dV$ $\quad \boldsymbol{B} = \nabla \times \boldsymbol{A}$
- Units of magnetic flux squared, i.e., Wb^2 in SI, Mx^2 in cgs
- Kinetic helicity in fluid dynamics (***B***→vorticity $\boldsymbol{\omega} = \nabla \times \boldsymbol{u}$),
  particle helicity in particle physics (the projection of the spin onto the direction of momentum)
- It is a geometrical measure of the twist and writhe of the magnetic field lines,
  and of the amount of flux linkages between pairs of lines (Gauss linking number)

single flux tube

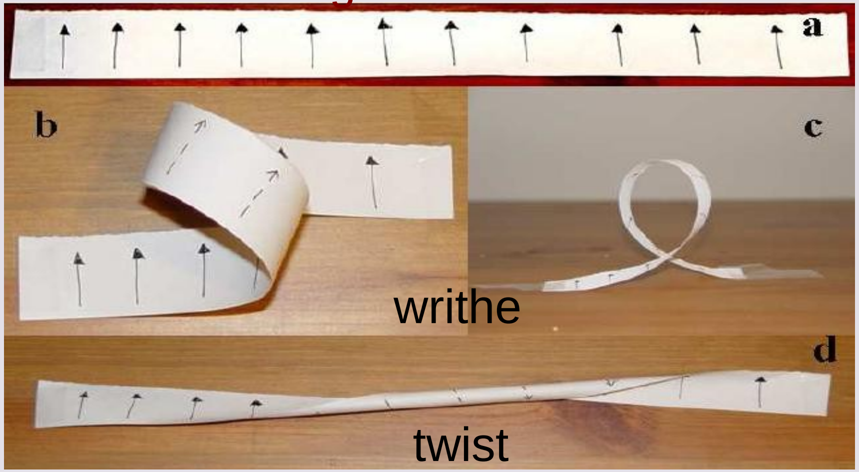

two closed flux tubes

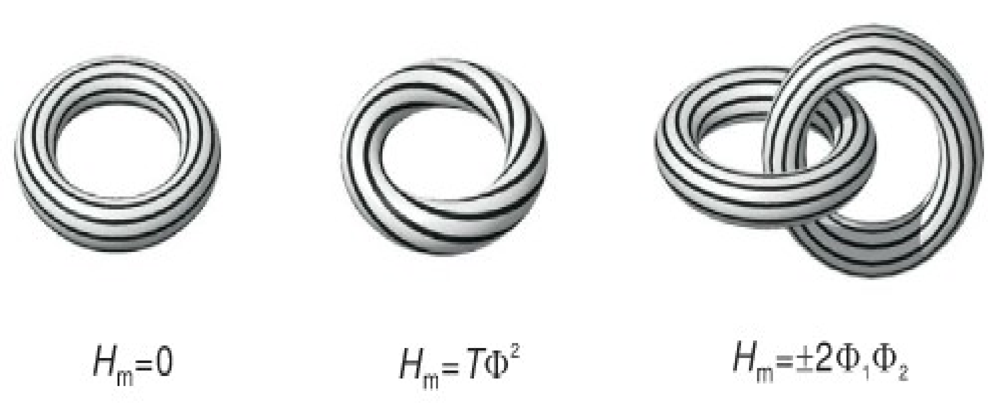

$$H = (Tw + Wr)\,\Phi^2$$

Why care?

- Conserved in ideal MHD (Woltjer 1958), along with energy and cross helicity

$$\frac{dH_m}{dt} = \int_{\partial\mathcal{V}} \left(\mathbf{A} \times \frac{\partial \mathbf{A}}{\partial t}\right) \cdot \mathrm{d}\mathbf{S} - 2\int_{\partial\mathcal{V}} (\mathbf{E} \times \mathbf{A}) \cdot \mathrm{d}\mathbf{S} - 2\int_{\mathcal{V}} \mathbf{E} \cdot \mathbf{B} \;\mathrm{d}\mathcal{V}$$

- Topological invariant; links cannot change by ‘frozen’ magnetic field lines
- Even in resistive MHD (reconnection), helicity is approximately conserved (Taylor 1975)
- Unlike energy, helicity goes to larger scales (inverse helicity cascade), and also dissipates slower than energy in non-ideal MHD
- In MHD turbulence, helicity bounds the energy distribution in the system

  $\mu_0 \hat{E}(k) > k\hat{H}(k)$ (Frisch et al. 1975)

- Linear force-free field = the minimum energy field for given helicity (Woltjer 1958)

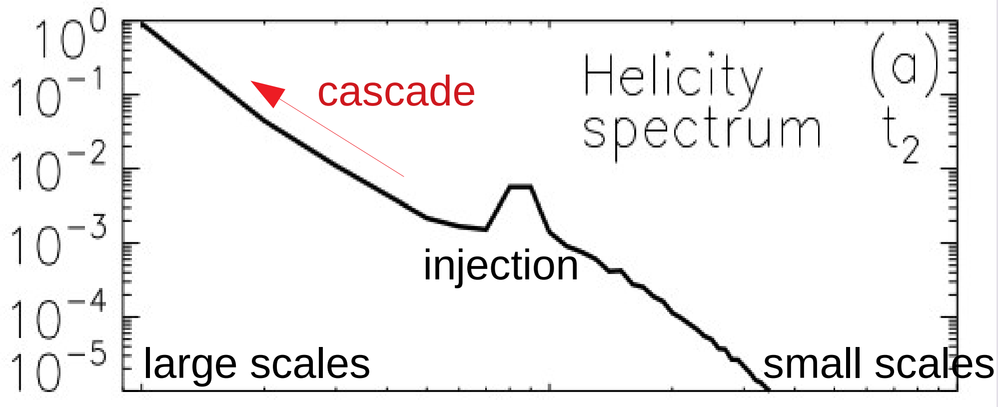

Alexakis et al. 2006

Applications

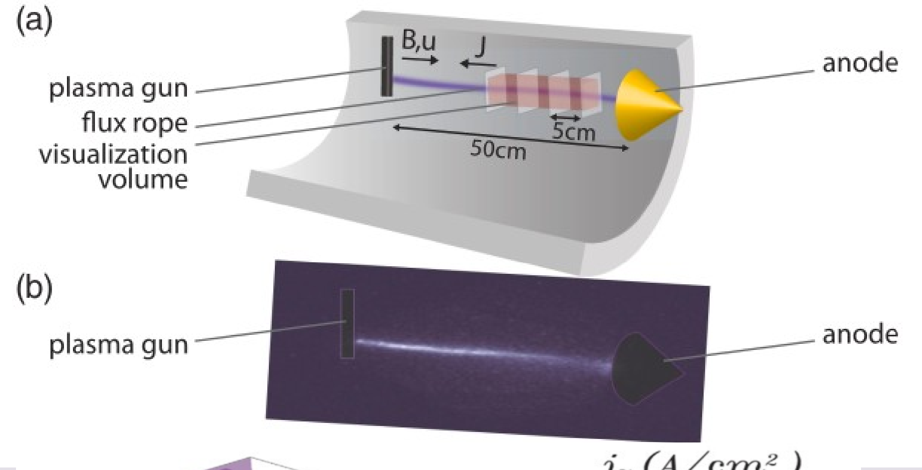

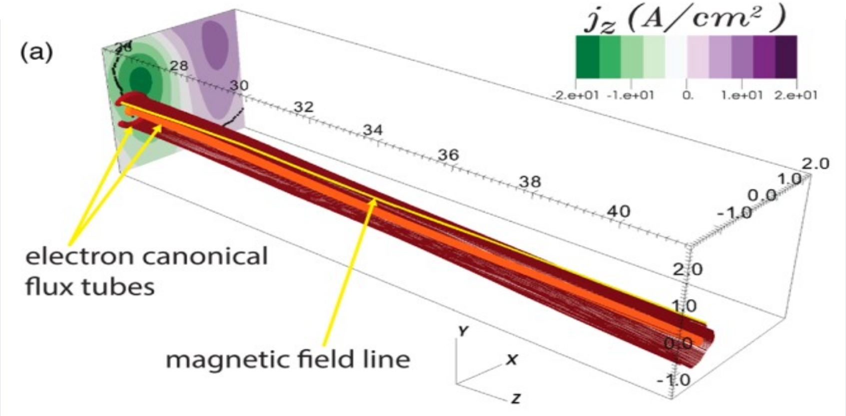

Plasma experiments

gyrating plasma kink: conversions between magnetic and kinetic energies in canonical flux tubes

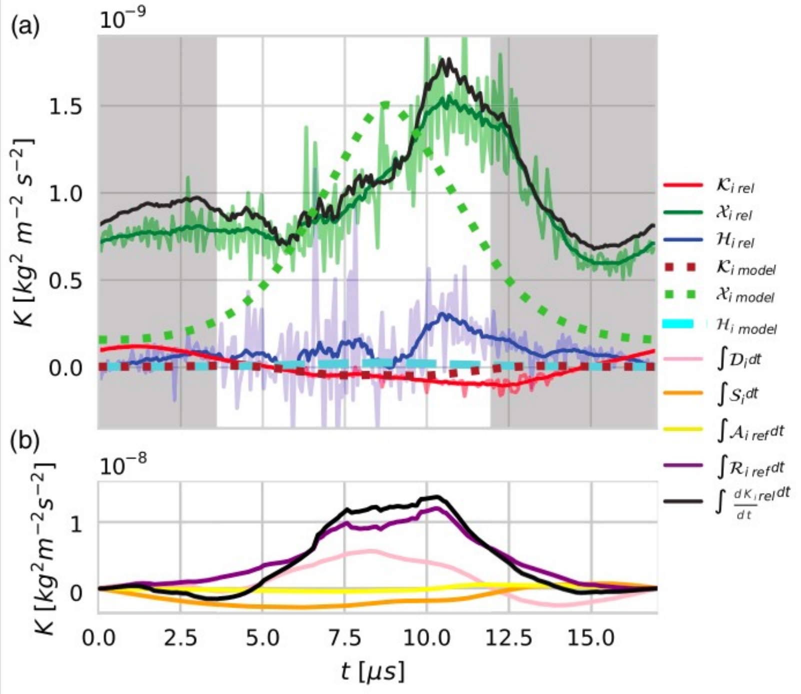

5 December 2018, Athens

von der Linden et al. 2018

Applications

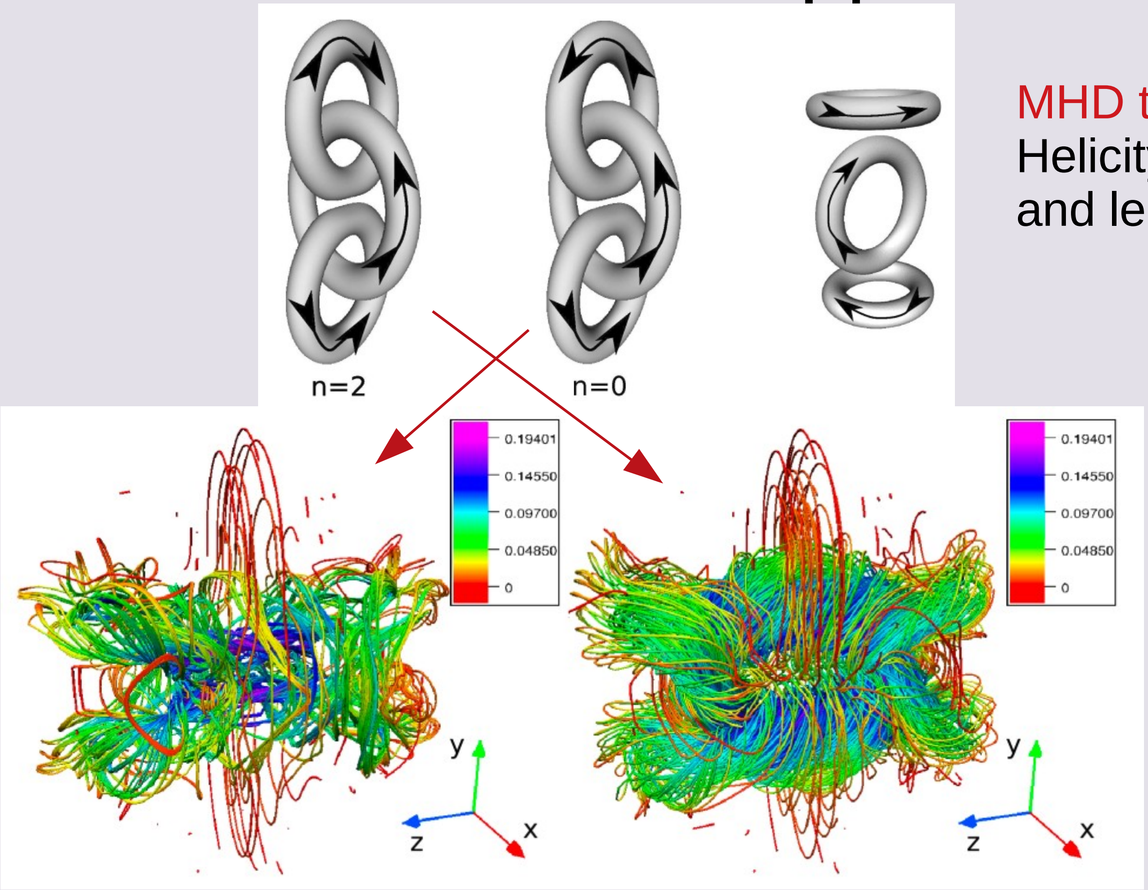

MHD turbulence

Helicity imposes restrictions on the relaxation, and leads to slower loss of magnetic energy

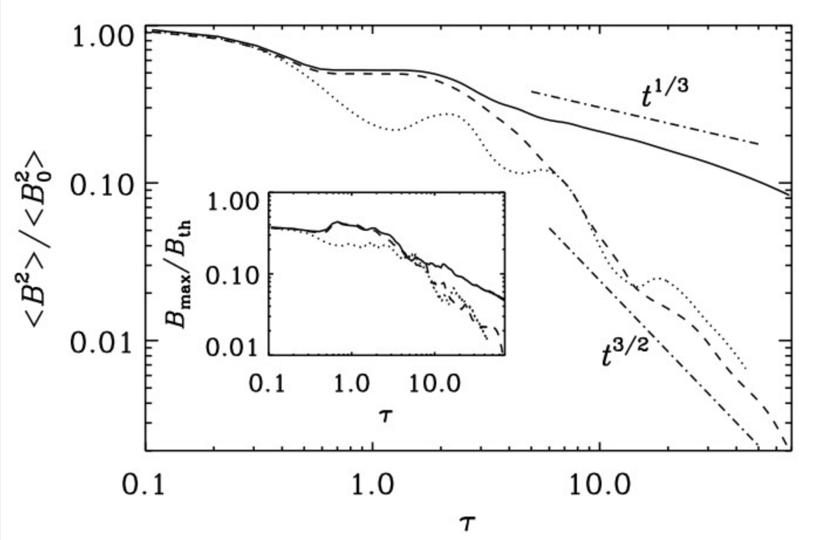

del Sordo et al. 2010

Applications

AGN jets

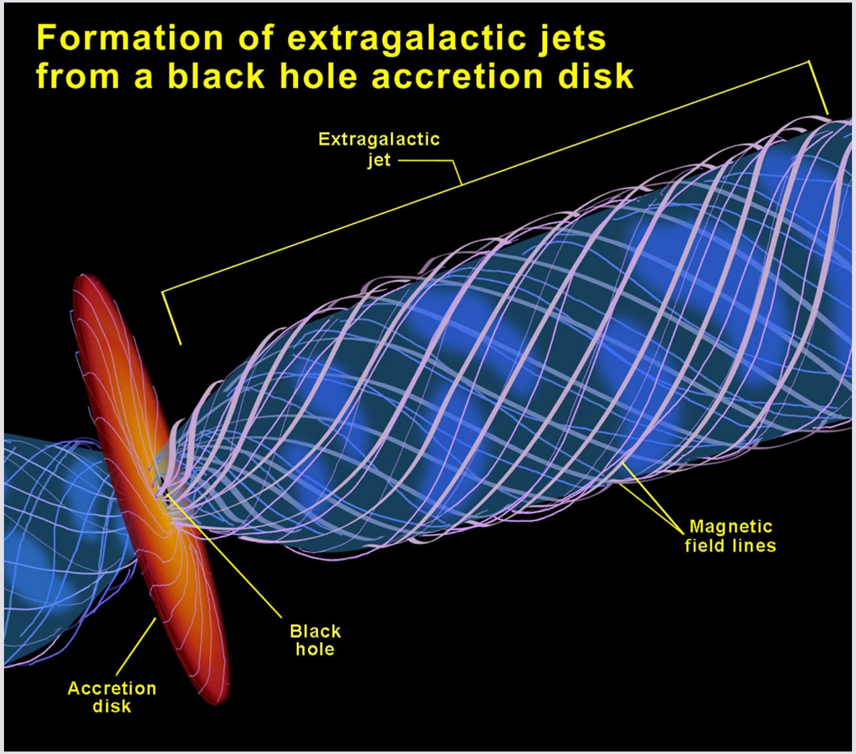

Galactic large-scale magnetic field
produced from dynamo mechanism

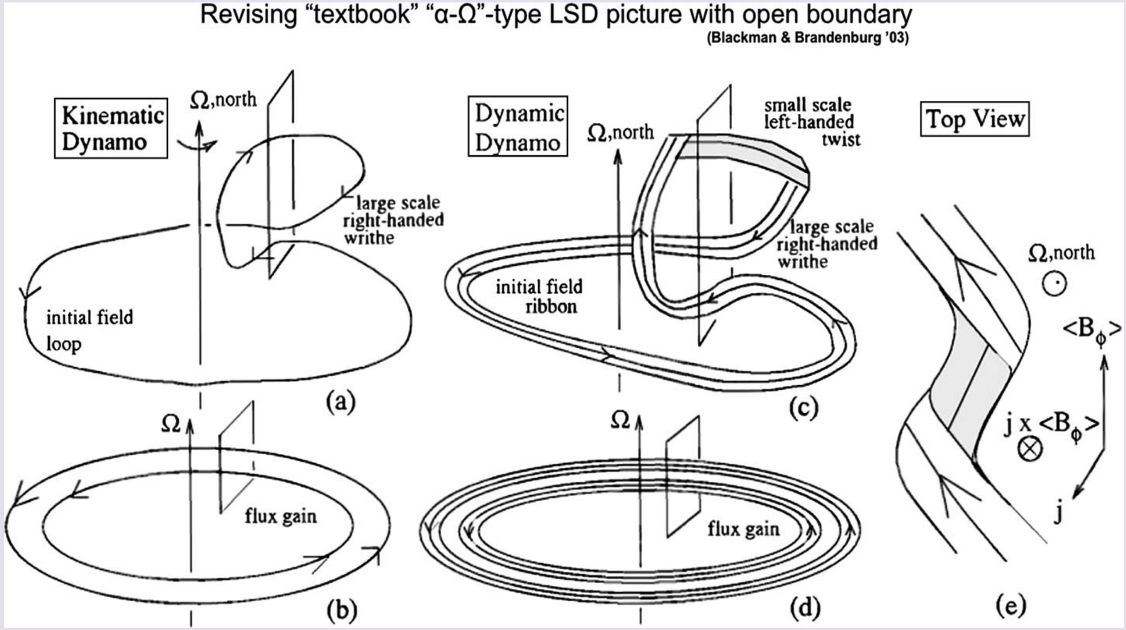

Applications

Radio bubbles in the intracluster medium
inflated by AGN outflows

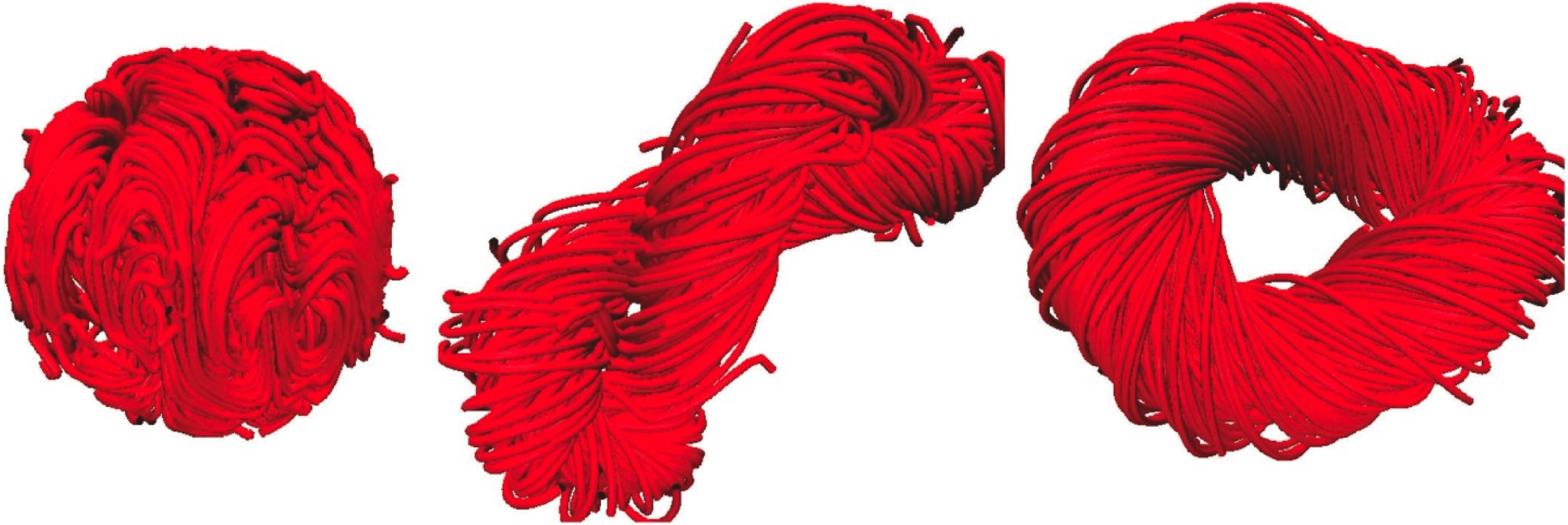

Braithwaite 2010

Applications

- Fundamental role of the magnetic field in the Sun
- Complex topology
- Coronal mass ejections are caused by the need to expel the excess helicity accumulated in the corona (Rust 1994)

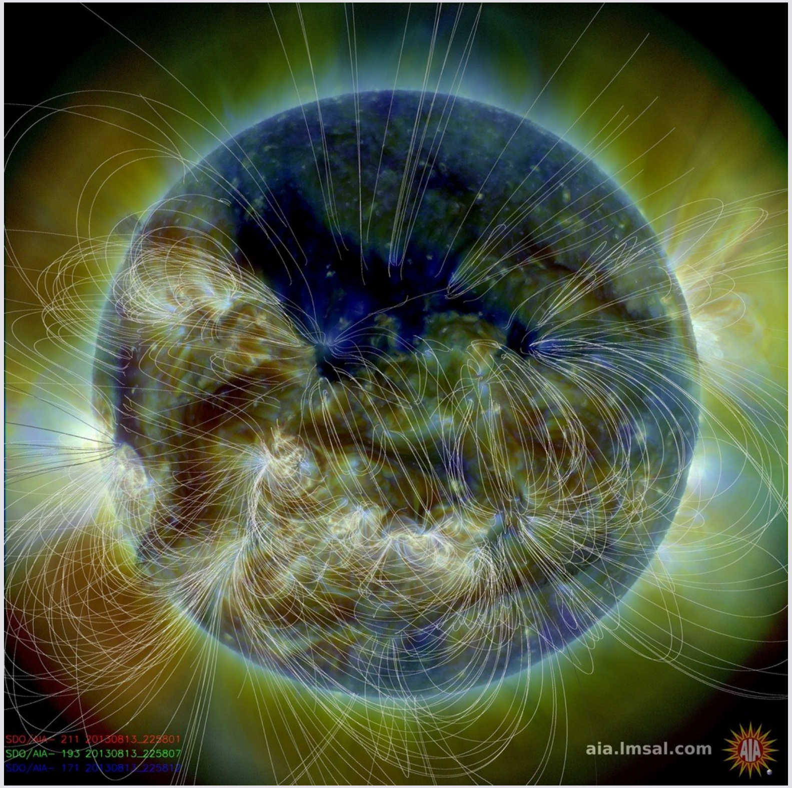

Applications

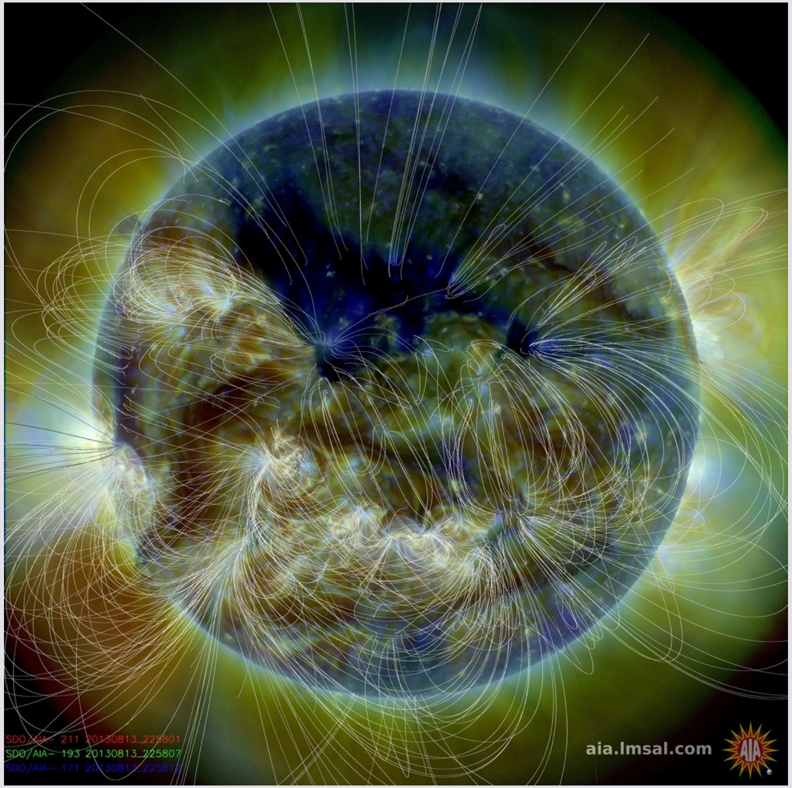

- Fundamental role of the magnetic field in the Sun
- Complex topology
- Coronal mass ejections are caused by the need to expel the excess helicity accumulated in the corona (Rust 1994)
- Helicity can provide eruptivity criteria

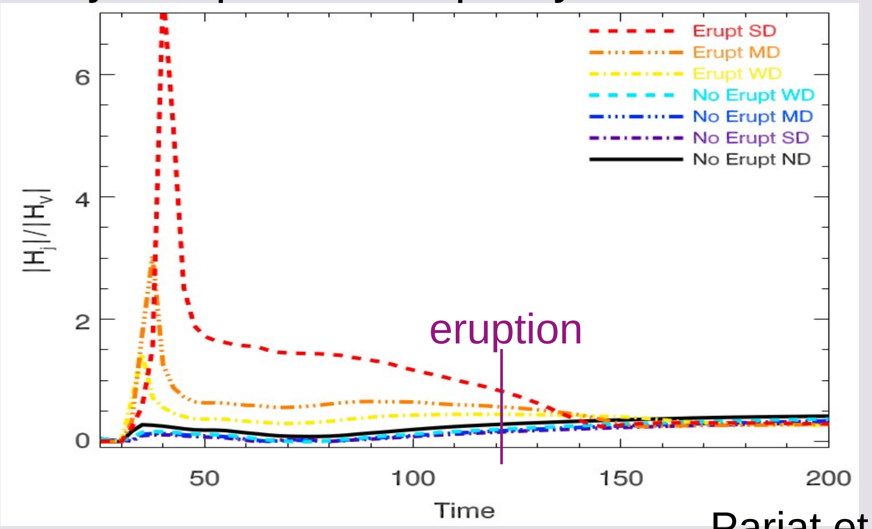

Pariat et al. 2017

Ok, what’s the catch?

Ok, what's the catch?

magnetic helicity

$$H=\int_V \boldsymbol{A}\cdot\boldsymbol{B}\,dV$$

under the gauge transformation

$$\boldsymbol{A}'=\boldsymbol{A}+\nabla\xi$$

becomes

$$H'=H+\oint \xi\,\boldsymbol{B}\cdot d\boldsymbol{S}$$

gauge independent for closed ***B***

$$\hat{n}\cdot\boldsymbol{B}\big|_{\partial V}=0$$

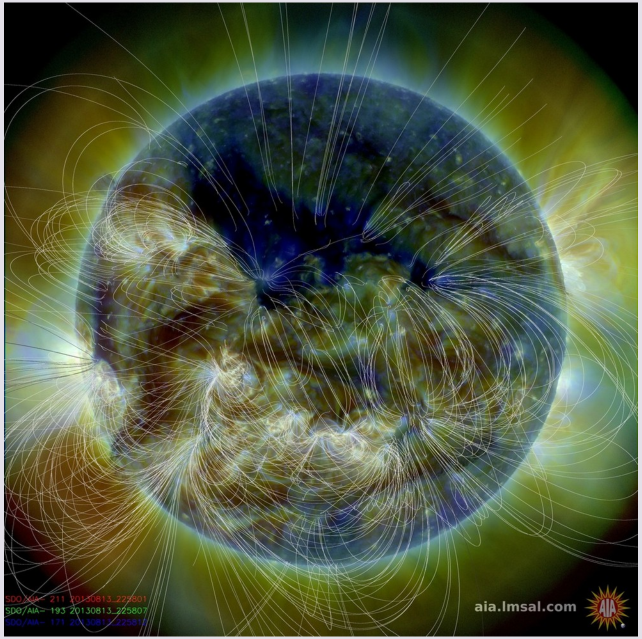

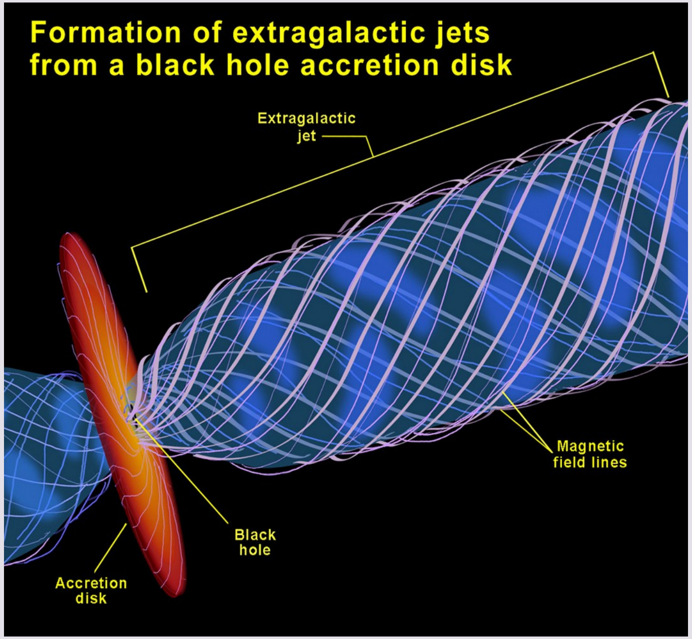

Relative magnetic helicity

magnetic helicity

$$H=\int_V \boldsymbol{A}\cdot\boldsymbol{B}\,dV$$

under the gauge transformation

$$\boldsymbol{A}'=\boldsymbol{A}+\nabla\xi$$

becomes

$$H'=H+\oint \xi\,\boldsymbol{B}\cdot d\boldsymbol{S}$$

gauge independent for closed ***B***

$$\hat{n}\cdot\boldsymbol{B}\big|_{\partial V}=0$$

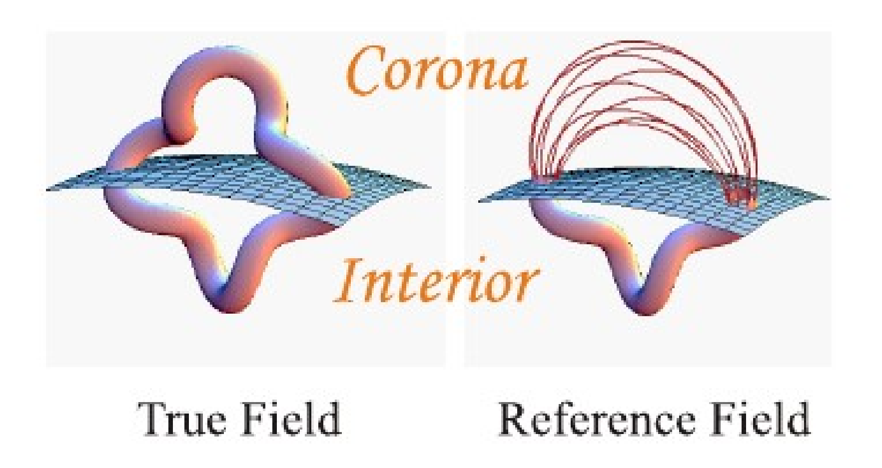

Berger & Field 1984, Finn & Antonsen 1985

relative magnetic helicity

$$H_r=\int_V (\mathbf{A}+\mathbf{A}_\mathrm{p})\cdot(\mathbf{B}-\mathbf{B}_\mathrm{p})\,dV$$

gauge independent for closed (and solenoidal) $\boldsymbol{B}-\boldsymbol{B}_p$

$$\hat{n}\cdot\boldsymbol{B}\big|_{\partial V}=\hat{n}\cdot\boldsymbol{B}_p\big|_{\partial V}$$

- ∂V: the whole boundary
- reference field=potential
- no current$\rightarrow$no helicity

RMH can uniquely be split into two gauge-invariant components H=H_j+H_{pj} following the splitting of the MF

$$\boldsymbol{B}=\boldsymbol{B}_p+\boldsymbol{B}_j$$

Outline

- Introduction
  - Magnetic helicity
    - Definition - Properties
  - Applications
  - Relative magnetic helicity
- Numerical computations of relative magnetic helicity
  - Cartesian geometry - Comparison with other methods
  - Spherical geometry
- Relative magnetic field line helicity
  - Definition - Validation
  - Visualization
- Conclusions

Computation of relative magnetic helicity

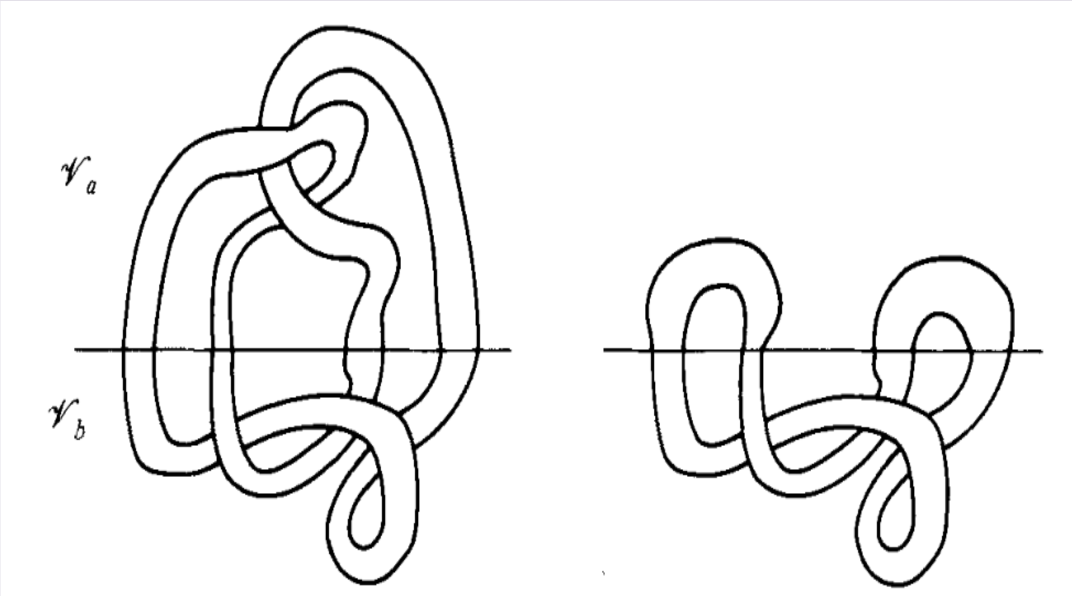

Definition: Berger & Field 1984
theoretical investigations

Computation of relative magnetic helicity

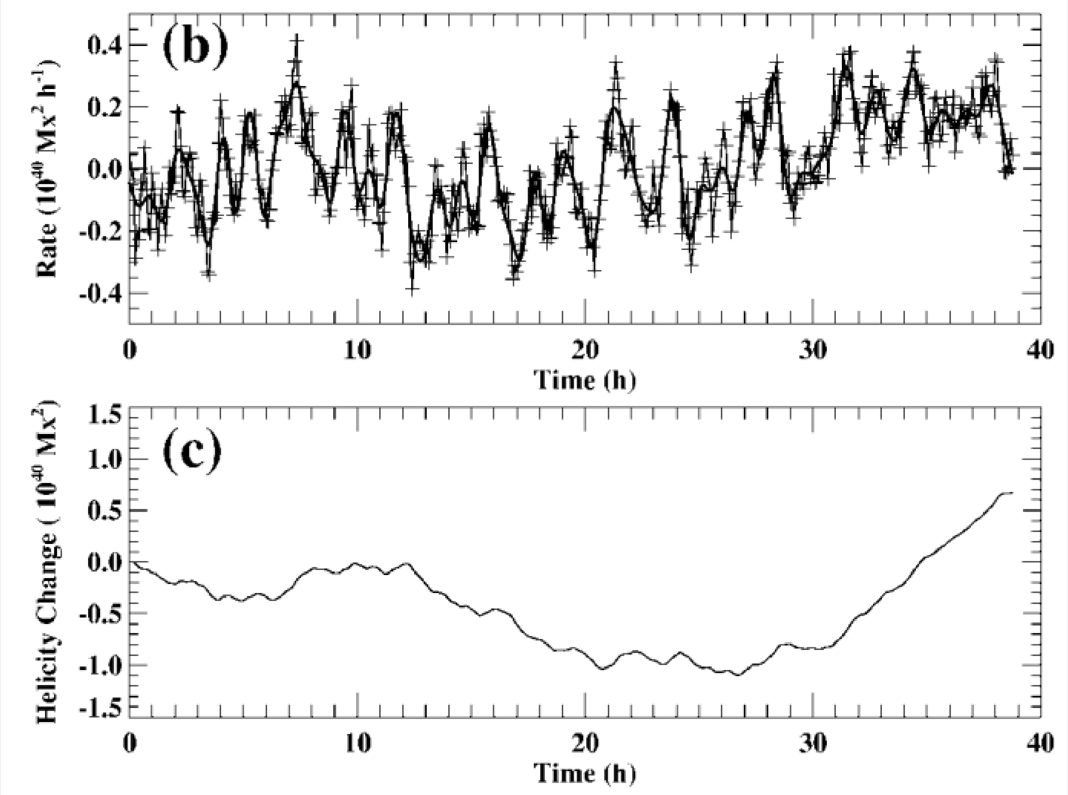

Definition: Berger & Field 1984
theoretical investigations

Observational determination: Chae 2001
many varieties developed
alternative approximate calculations

Computation of relative magnetic helicity

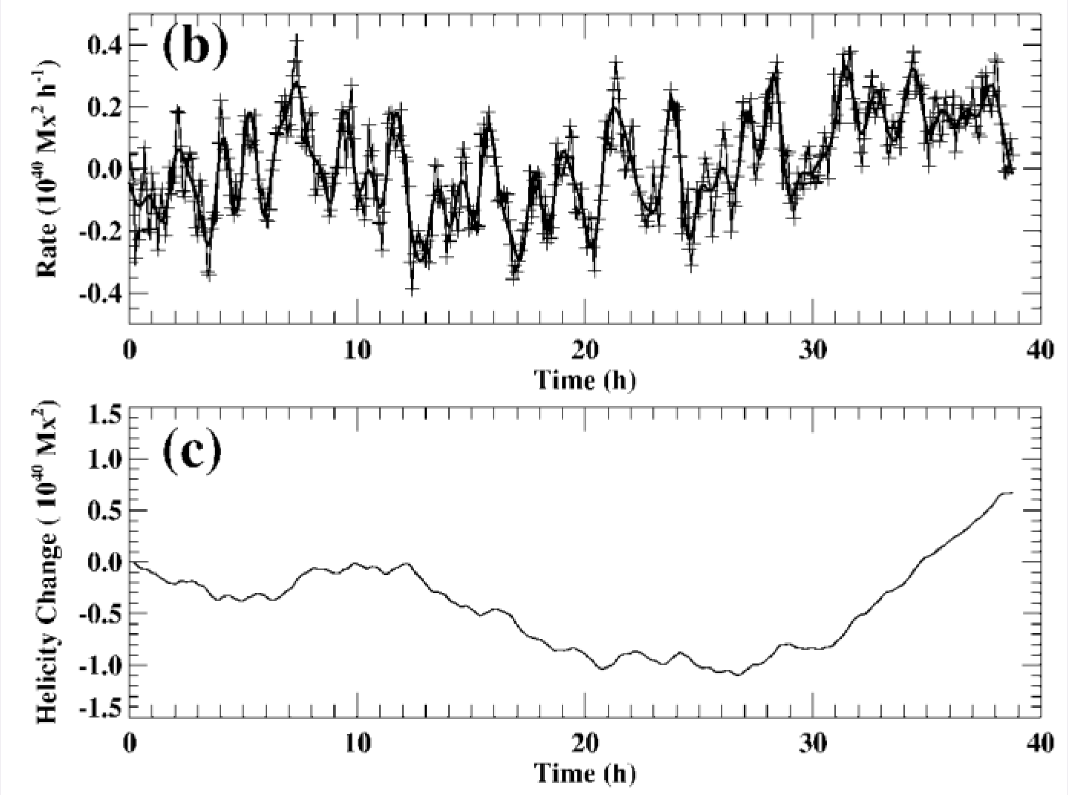

Definition: Berger & Field 1984
theoretical investigations

Observational determination: Chae 2001
many varieties developed
alternative approximate calculations

Computation in a Cartesian box:
Thalmann et al. 2011
Rudenko & Myshyakov 2011
Valori et al. 2012
Yang et al. 2013
Moraitis et al. 2014

Computation of relative magnetic helicity

Table 1 Synoptic view of helicity computation methods, their properties and formulation, as described in Sect. 1.2. The subset of methods actually tested in this paper is listed in Table 2

Finite volume (FV)

$$\mathcal{H}_{\mathcal{V}} = \int_{\mathcal{V}} (\mathbf{A}+\mathbf{A}_{\mathrm{p}}) \cdot (\mathbf{B}-\mathbf{B}_{\mathrm{p}})\, \mathrm{d}\mathcal{V}$$

see Eq. (3)

- Requires $\mathbf{B}$ in $\mathcal{V}$ *e.g.*, from MHD simulations or NLFFF
- Compute $\mathcal{H}_{\mathcal{V}}$ at one time
- May employ different gauges (see Table 2)

Helicity-flux integration (FI)

$$\frac{\mathrm{d}\mathcal{H}_{\mathcal{V}}}{\mathrm{d}t} = 2 \int_{\partial\mathcal{V}} [(\mathbf{A}_{\mathrm{p}} \cdot \mathbf{B}) v_n - (\mathbf{A}_{\mathrm{p}} \cdot \mathbf{v}_{\mathrm{t}}) B_n]\, \mathrm{d}S$$

- Requires time evolution of vector field on $\partial\mathcal{V}$
- Requires knowledge or model of flows on $\partial\mathcal{V}$
- Valid for a specific set of gauge and assumptions, see Pariat et al. (2017)

Discrete flux-tubes (DT)

$$\mathcal{H} \simeq \sum_{i=1}^{M} \mathcal{T}_i \Phi_i^2 + \sum_{i=1}^{M} \sum_{j=1, j\neq i}^{M} \mathcal{L}_{i,j} \Phi_i \Phi_j ,$$

see Eq. (31)

Twist-number (TN)

$$\mathcal{H} \simeq \mathcal{T} \Phi^2$$

see Eq. (32)

- Estimation of the twist contribution to $\mathcal{H}$
- Requires $\mathbf{B}$ in $\mathcal{V}$
- Requires a flux-rope-like structure for computing the twist $\mathcal{T}$

Connectivity-based (CB)

$$\mathcal{H} = A \sum_{i=1}^{M} \alpha_i \Phi_i^{2\delta} + \sum_{l,m=1}^{M} \mathcal{L}_{lm} \Phi_l \Phi_m$$

see Eq. (35)

- Requires the vector field on photosphere at one time
- Models the corona connectivity as a collection of M force-free flux tubes
- Minimal connection length principle

Finite-volume methods

1. given $\boldsymbol{B}$ find $\boldsymbol{B}_{\mathrm{p}}$
2. given $\boldsymbol{B}$, $\boldsymbol{B}_{\mathrm{p}}$ find $\boldsymbol{A}$, $\boldsymbol{A}_{\mathrm{p}}$

$$H_r = \int_V (\mathbf{A}+\mathbf{A}_{\mathrm{p}}) \cdot (\mathbf{B}-\mathbf{B}_{\mathrm{p}})\, dV$$

Moraitis et al. 2014

Valori et al. 2016, Space Science Reviews

Computation in Cartesian case

Step 1 – Potential field calculation

Potential magnetic field satisfying condition

$$\mathbf{B}_\mathrm{p} = \nabla\Phi$$
$$\hat{n}\cdot\mathbf{B}_\mathrm{p}|_{\partial V} = \hat{n}\cdot\mathbf{B}|_{\partial V}$$

→

$$\nabla^2\Phi = 0$$
$$\left.\frac{\partial\Phi}{\partial\hat{n}}\right|_{\partial V} = \hat{n}\cdot\mathbf{B}|_{\partial V}$$

solution of Laplace's equation under Neumann BCs

$$\frac{\partial^2\Phi}{\partial x^2} + \frac{\partial^2\Phi}{\partial y^2} + \frac{\partial^2\Phi}{\partial z^2} = 0$$
$$\left.\frac{\partial\Phi}{\partial\hat{n}}\right|_{\partial V} = \hat{n}\cdot\mathbf{B}|_{\partial V}$$

in the finite volume

$$V = \{(x,y,z) : x\in[x_0,x_1],\ y\in[y_0,y_1],\ z\in[z_0,z_1]\}$$

- BVP well defined only for flux-balanced magnetic fields
- FORTRAN routine HW3CRT from FISHPACK library (or D03FAF from NAG)
- Routine uses FFT method in non-homogeneous, uniform grid
- For non-uniform grid interpolation to and from a uniform grid is required

Computation in Cartesian case

Step 2 – Vector potentials calculation

invert $\mathbf{B} = \nabla \times \mathbf{A}$ with Valori et al. (2012) method

DeVore (2000) gauge $\hat{\mathbf{z}} \cdot \mathbf{A} = 0$

$$\mathbf{A}(x, y, z) = \boldsymbol{\alpha}(x, y) + \hat{\mathbf{z}} \times \int_{z_0}^{z} \mathrm{d}z' \, \mathbf{B}(x, y, z')$$

$$\nabla_\perp \times \boldsymbol{\alpha} = B_z(x, y, z_0)$$

Simple gauge

$$\alpha_y(x, y) = c \int_{x_0}^{x} \mathrm{d}x' \, B_z(x', y, z_0)$$

$$\alpha_x(x, y) = -(1 - c) \int_{y_0}^{y} \mathrm{d}y' \, B_z(x, y', z_0)$$

$$c \in [0, 1]$$

Coulomb gauge

$$\nabla_\perp \cdot \boldsymbol{\alpha} = 0 \qquad \boldsymbol{\alpha} = \hat{\mathbf{z}} \times \nabla_\perp u$$

$$\nabla_\perp^2 u = B_z(x, y, z_0)$$

- Same method for both vector potentials
- Integrations: modified Simpson or trapezoidal rule, applicable also to non-uniform grid
- Top/bottom reference planes give different results – top is usually better
- 2D Poisson problem: FORTRAN routine HWSCRT from FISHPACK library using FFT method in non-homogeneous, uniform grid
- For non-uniform grid interpolation to and from a uniform grid is required

Comparison with other methods

Magnetic Helicity estimations in models and observations of the solar magnetic field

ISSI Team led by Gherardo Valori (MSSL - UK) & Etienne Pariat (LESIA - France)

Search

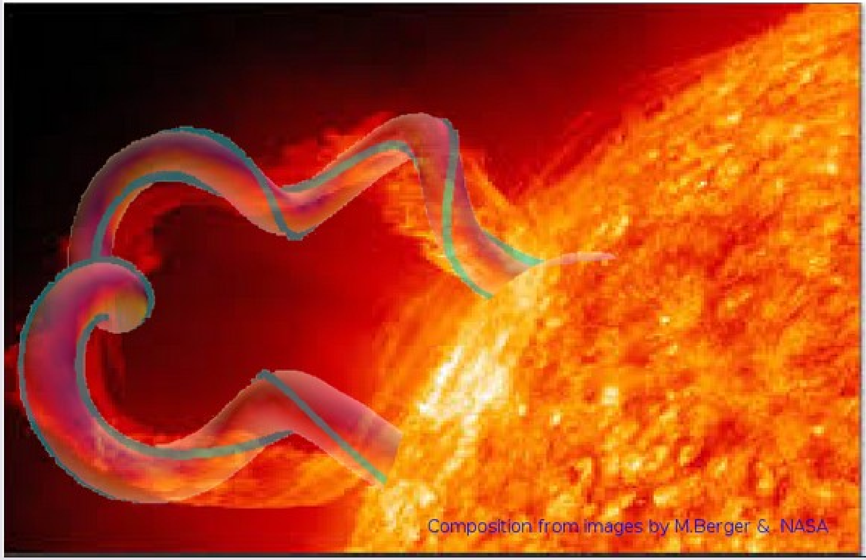

INTERNATIONAL
SPACE
SCIENCE
INSTITUTE

International Team on

Magnetic Helicity

Comparison with other methods

Space Sci Rev (2016) 201:147–200
DOI 10.1007/s11214-016-0299-3

CrossMark

Magnetic Helicity Estimations in Models and Observations of the Solar Magnetic Field. Part I: Finite Volume Methods

Gherardo Valori[1] · Etienne Pariat[2] · Sergey Anfinogentov[3] · Feng Chen[4] · Manolis K. Georgoulis[5] · Yang Guo[6] · Yang Liu[7] · Kostas Moraitis[5] · Julia K. Thalmann[8] · Shangbin Yang[9]

Comparison with other methods

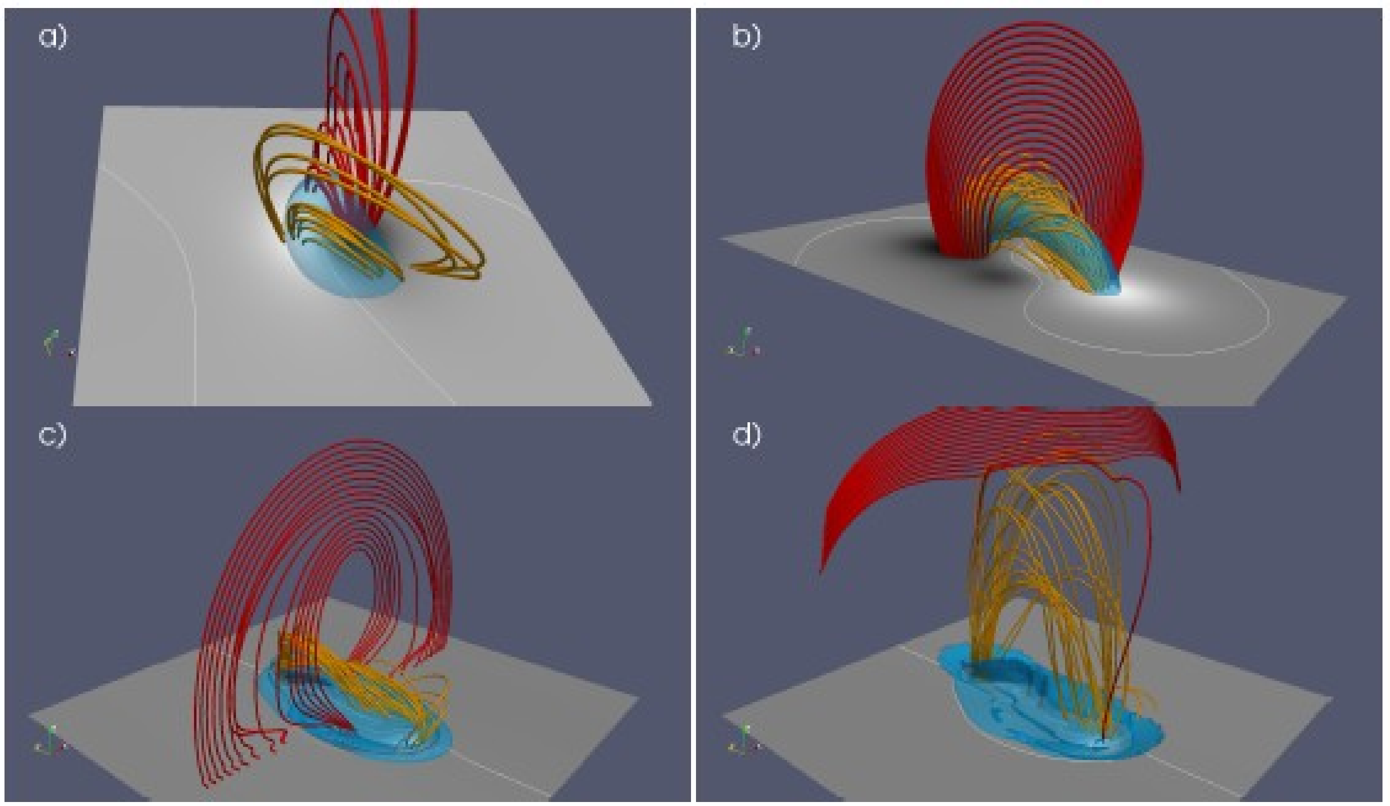

- Low & Lou @ 4 resolutions
- TD different twist and/or resolution
- Stable MHD simulation Leake et al. 2013
- Unstable MHD simulation Leake et al. 2014

Comparison with other methods

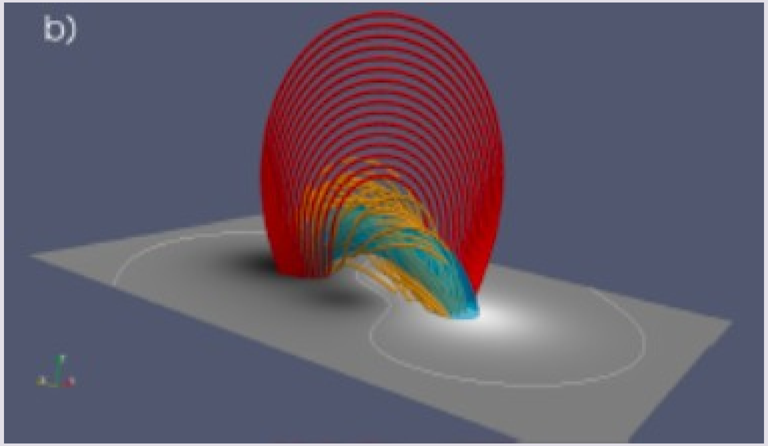

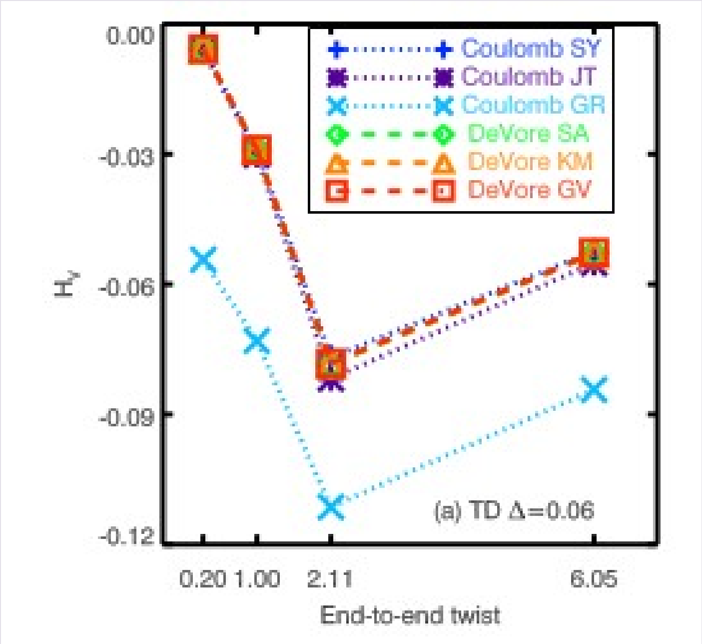

- All methods (except GR) within 2%
- DeVore gauge more accurate than Coulomb gauge
- More twist isn't more helicity

Comparison with other methods

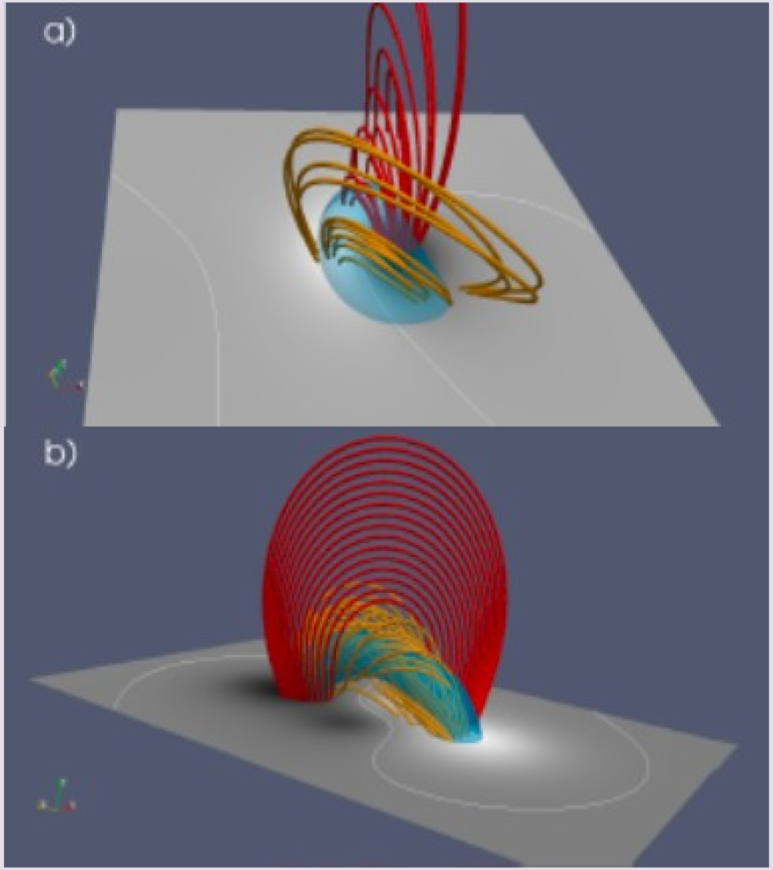

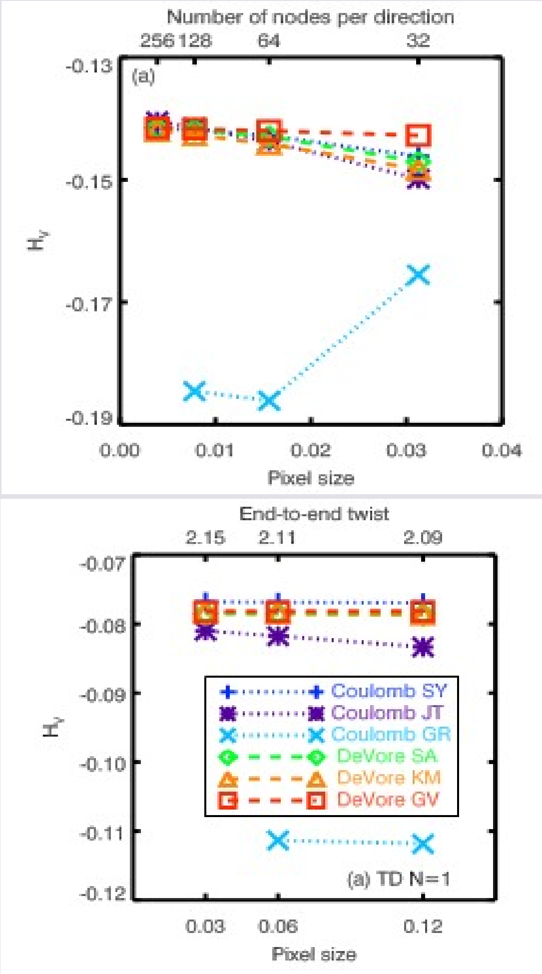

- Weak dependence on resolution in TD, but more clear in LL
- Spread within 4%
- Differences between methods more important
- Lower resolution = more B divergence

Comparison with other methods

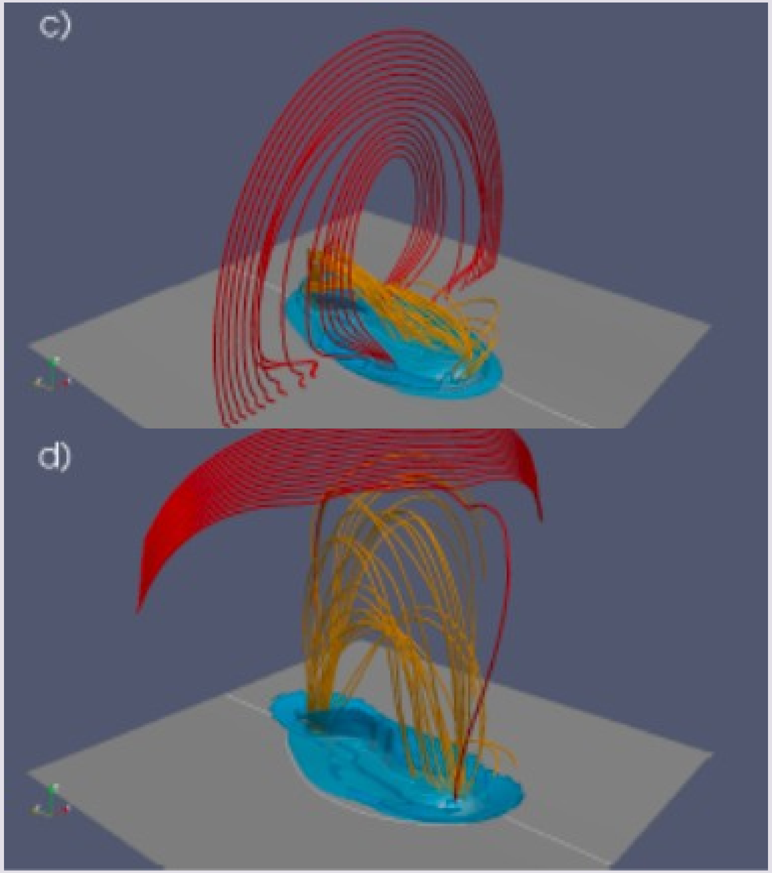

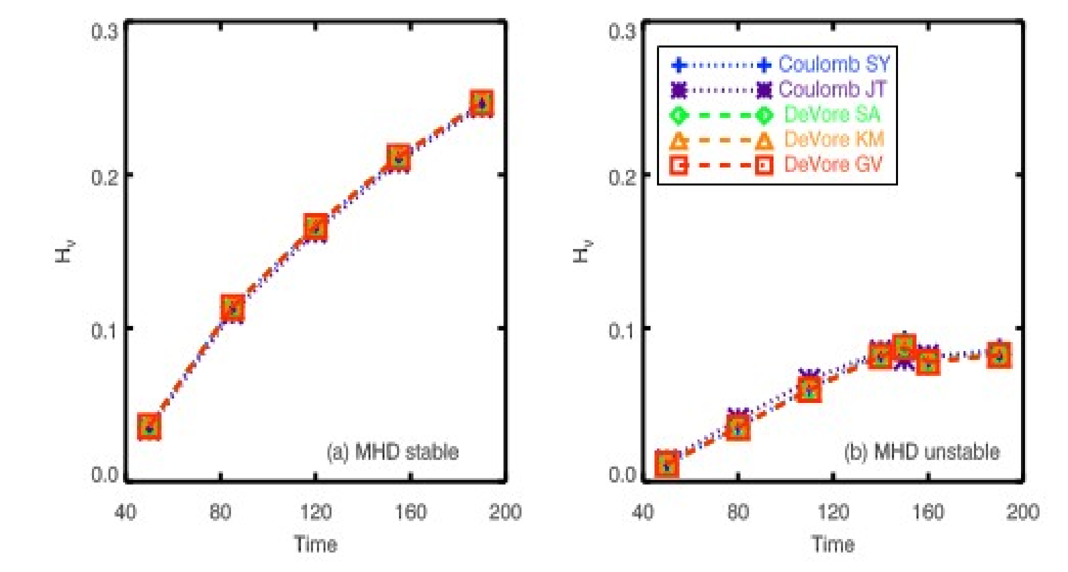

- Spread in helicity values 0.2% (st) and 3% (un)
- More helicity isn't more eruptive

Comparison with other methods

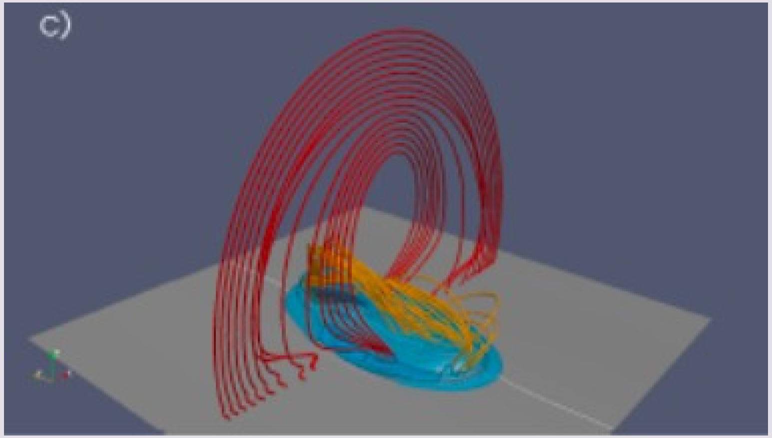

Split ***B*** (of MHD-st at t=50) in solenoidal and non-solenoidal parts (Valori et al. 2013), then add ns in controlled way

$$\boldsymbol{B}_\delta = \boldsymbol{B}_s + \delta\, \boldsymbol{B}_{ns}$$

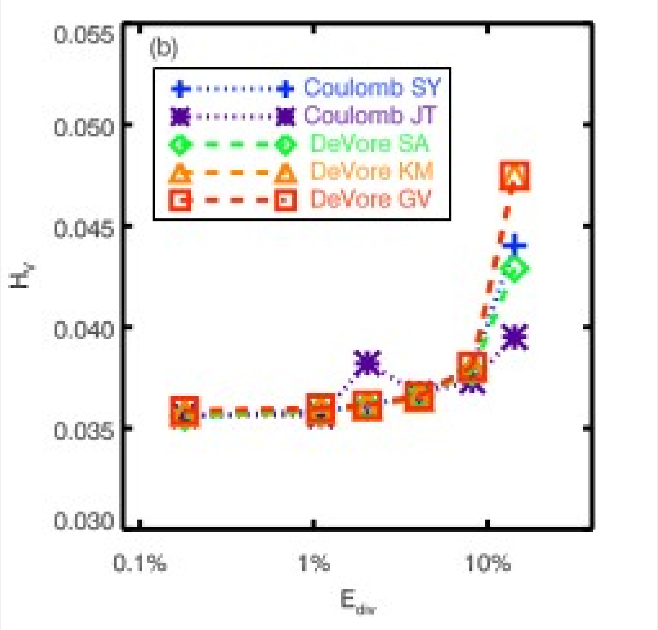

- Spread in helicity values grows from 1% to 20%
- Max reasonable helicity for divergence errors <~8%

Computation in spherical case

Finite-volume methods

1. given ***B*** find ***B***$_\mathbf{p}$
2. given ***B***, ***B***$_\mathbf{p}$ find ***A***, ***A***$_\mathbf{p}$

$$H_r = \int_V (\mathbf{A} + \mathbf{A}_\mathrm{p}) \cdot (\mathbf{B} - \mathbf{B}_\mathrm{p}) \, dV$$

Moraitis et al. 2018

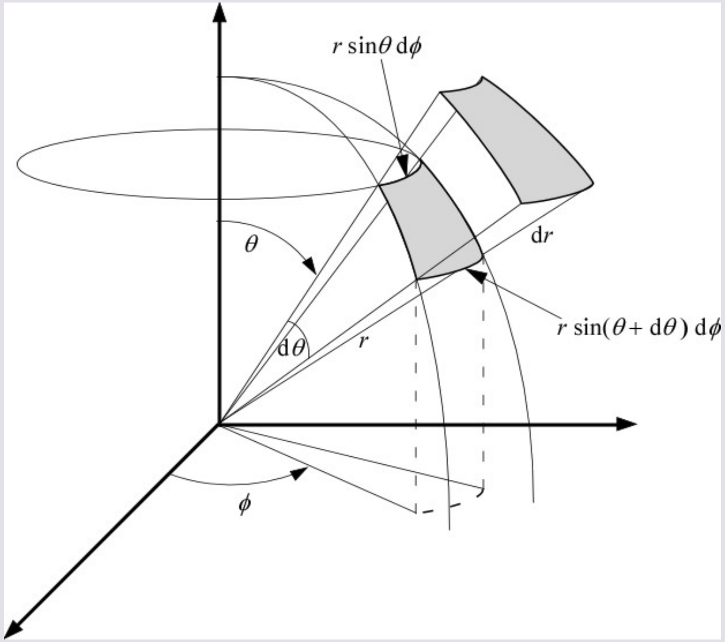

Computation in spherical case

Step 1 – Potential field calculation

Potential magnetic field satisfying condition

$$\mathbf{B}_\mathrm{p} = \nabla\Phi$$
$$\hat{n}\cdot\mathbf{B}_\mathrm{p}|_{\partial V} = \hat{n}\cdot\mathbf{B}|_{\partial V}$$

→

$$\nabla^2\Phi = 0$$
$$\left.\frac{\partial\Phi}{\partial\hat{n}}\right|_{\partial V} = \hat{n}\cdot\mathbf{B}|_{\partial V}$$

solution of Laplace's equation under Neumann BCs

$$\frac{1}{r^2}\frac{\partial}{\partial r}\left(r^2\frac{\partial\Phi}{\partial r}\right) + \frac{1}{r^2\sin\theta}\frac{\partial}{\partial\theta}\left(\sin\theta\frac{\partial\Phi}{\partial\theta}\right) + \frac{1}{r^2\sin\theta^2}\frac{\partial^2\Phi}{\partial\phi^2} = 0$$
$$\left.\frac{\partial\Phi}{\partial\hat{n}}\right|_{\partial V} = \hat{n}\cdot\mathbf{B}|_{\partial V}$$

in the finite volume

$$V = \{(r,\theta,\phi) : r\in[r_0,r_1],\, \theta\in[\theta_0,\theta_1],\, \phi\in[\phi_0,\phi_1]\}$$

- BVP well defined only for flux-balanced magnetic fields
- FORTRAN routine MUD3SA from MUDPACK library
- Routine uses multigrid method in non-homogeneous, uniform grid of special form $m*2^{n-1}+1$, m, n integers, and positive φ
- For non-uniform/non-special grid interpolation to and from a uniform/special grid is required

Computation in spherical case

Step 2 – Vector potentials calculation

invert $\mathbf{B} = \nabla \times \mathbf{A}$ with Valori et al. (2012) method

DeVore (2000) gauge $\hat{\mathbf{r}} \cdot \mathbf{A} = 0$

$$\mathbf{A}(r,\theta,\phi) = \frac{1}{r}\left(r_0 \boldsymbol{\alpha}(\theta,\phi) + \hat{\mathbf{r}} \times \int_{r_0}^{r} \mathrm{d}r' \, r' \mathbf{B}(r',\theta,\phi)\right)$$

$$\nabla_\perp \times \boldsymbol{\alpha} = B_r(r_0,\theta,\phi)$$

Simple gauge

$$\alpha_\phi(\theta,\phi) = \frac{c r_0}{\sin\theta} \int_{\theta_0}^{\theta} \mathrm{d}\theta' \, \sin\theta' B_r(r_0,\theta',\phi)$$

$$\alpha_\theta(\theta,\phi) = -(1-c) r_0 \sin\theta \int_{\phi_0}^{\phi} \mathrm{d}\phi' \, B_r(r_0,\theta,\phi')$$

$$c \in [0,1]$$

Coulomb gauge

$$\nabla_\perp \cdot \boldsymbol{\alpha} = 0 \qquad \boldsymbol{\alpha} = \hat{\mathbf{r}} \times \nabla_\perp u$$

$$\nabla_\perp^2 u = B_r(r_0,\theta,\phi)$$

- Same method for both vector potentials
- Integrations: trapezoidal rule, applicable also to non-uniform grid
- Top/bottom reference planes give different results – top is usually better
- 2D Poisson problem: FORTRAN routine HWSSSP from FISHPACK library using FFT method in non-homogeneous, uniform grid
- For non-uniform grid interpolation to and from a uniform grid is required

Computation in spherical case

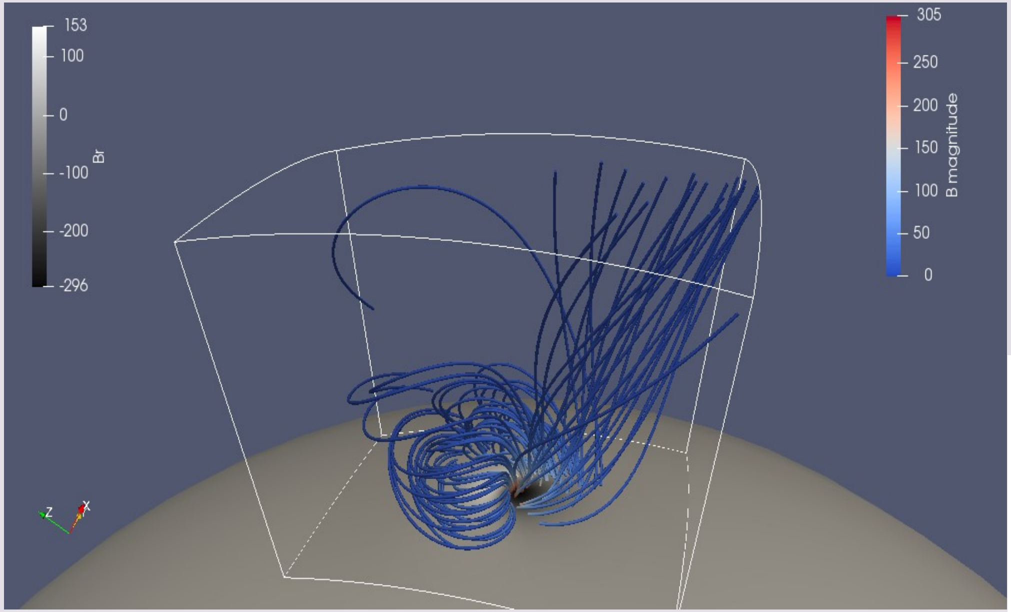

Validation against semi-analytic NLFF fields of Low & Lou (1990) with:

- different resolution
- different reference plane
- different gauge

Table 2 Metrics for the reconstruction of the magnetic field from the respective vector potential.

Field	Gauge	Grid	Correlation coefficients of $\boldsymbol{B}$ *vs.* $\nabla \times \boldsymbol{A}$			Schrijver metrics				
			B_r	B_θ	B_ϕ	C_{vec}	C_{CS}	E'_{n}	E'_{m}	ϵ
$\boldsymbol{B}_{\mathrm{LL}}$	DVSt	129^3	0.9999	1.0000	1.0000	0.9999	1.0000	0.9948	0.9959	0.9980
	DVSt	257^3	0.9999	1.0000	1.0000	0.9999	1.0000	0.9942	0.9949	0.9986
	DVSb	129^3	0.9990	1.0000	1.0000	0.9995	0.9986	0.9814	0.9613	1.0025
	DVCt	129^3	0.9999	1.0000	1.0000	0.9999	0.9999	0.9947	0.9953	0.9980
$\boldsymbol{B}_{\mathrm{p,LL}}$	DVSt	129^3	1.0000	1.0000	1.0000	1.0000	0.9998	0.9888	0.9829	0.9977
	DVSt	257^3	0.9995	1.0000	1.0000	0.9997	0.9962	0.9570	0.9288	0.9990
	DVSb	129^3	0.9999	1.0000	1.0000	0.9999	0.9978	0.9843	0.9627	1.0008
	DVCt	129^3	1.0000	1.0000	1.0000	1.0000	0.9997	0.9888	0.9824	0.9977

Outline

- Introduction
  - Magnetic helicity
    - Definition - Properties
  - Applications
  - Relative magnetic helicity
- Numerical computations of relative magnetic helicity
  - Cartesian geometry - Comparison with other methods
  - Spherical geometry
- Relative magnetic field line helicity
  - Definition - Validation
  - Visualization
- Conclusions

Field line helicity

Definition: The integral of the vector potential along a field line

$$\mathcal{A}(C;\mathbf{A}) = \begin{cases} \int_{\alpha_+}^{\alpha_-} \mathbf{A}\cdot d\boldsymbol{l}, & C \text{ open} \\ \oint_C \mathbf{A}\cdot d\boldsymbol{l}, & C \text{ closed} \end{cases}$$

+ : Magnetic helicity then reduces to a surface integral along the boundary

$$H = \int_{\partial V} \mathcal{A}\, d\Phi$$

- : FLH is gauge-dependent
not properly defined for relative magnetic helicity

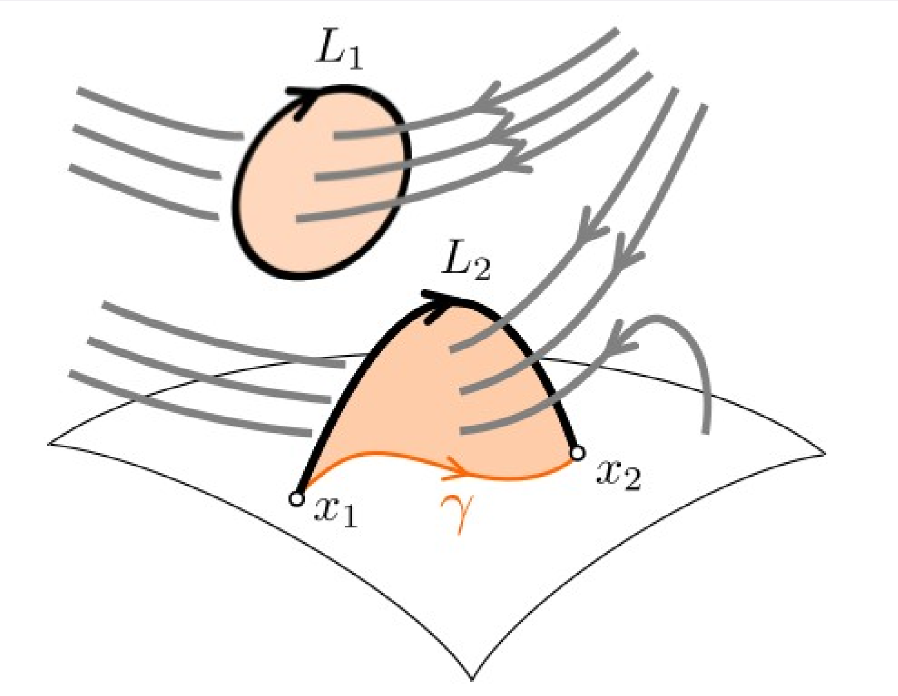

Yeates & Hornig 2016

Relative magnetic field line helicity

$$H_r = \int_V (\mathbf{A} + \mathbf{A}_\mathrm{p}) \cdot (\mathbf{B} - \mathbf{B}_\mathrm{p})\, dV$$

$$H_r = \int_V (\mathbf{A} + \mathbf{A}_\mathrm{p}) \cdot \mathbf{B}\, dV - \int_V (\mathbf{A} + \mathbf{A}_\mathrm{p}) \cdot \mathbf{B}_\mathrm{p}\, dV$$

$$H_r = \int_{\partial V+} |\hat{n} \cdot \mathbf{B}| \left(\int_{\alpha_+}^{\alpha_-} (\mathbf{A} + \mathbf{A}_\mathrm{p}) \cdot dl \right) dS - \int_{\partial V+} |\hat{n} \cdot \mathbf{B}_\mathrm{p}| \left(\int_{\alpha_{p+}}^{\alpha_{p-}} (\mathbf{A} + \mathbf{A}_\mathrm{p}) \cdot dl_\mathrm{p} \right) dS$$

$$H_r = \int_{\partial V+} |\hat{n} \cdot \mathbf{B}| \left(\int_{\alpha_+}^{\alpha_-} (\mathbf{A} + \mathbf{A}_\mathrm{p}) \cdot dl - \int_{\alpha_+}^{\alpha_{p-}} (\mathbf{A} + \mathbf{A}_\mathrm{p}) \cdot dl_\mathrm{p} \right) dS$$

$$H_r = \int_{\partial V+} \mathcal{A}_r^+ \, d\Phi$$

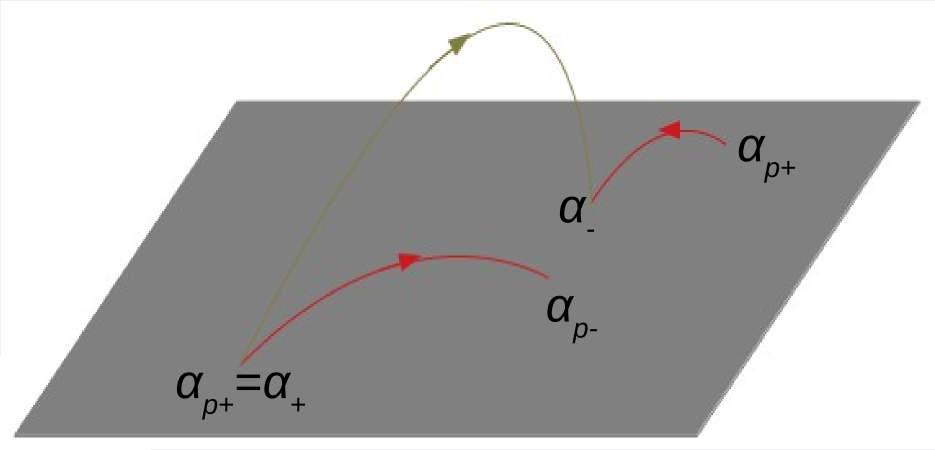

flux-tube assumption

$$\partial V^\pm = \{\mathbf{x} \in \partial V : \hat{n} \cdot \mathbf{B}(\mathbf{x}) \lessgtr 0\}$$

start from same footpoint $\alpha_{p+}=\alpha_+$

so that $|\hat{n} \cdot \mathbf{B}| = |\hat{n} \cdot \mathbf{B}_\mathrm{p}|$

Moraitis et al. 2018 (under review)

Relative magnetic field line helicity

$$\mathcal{A}_r^{+} = \int_{\alpha_+}^{\alpha_-} (\mathbf{A}+\mathbf{A}_\mathrm{p})\cdot d\boldsymbol{l} - \int_{\alpha_+}^{\alpha_{p-}} (\mathbf{A}+\mathbf{A}_\mathrm{p})\cdot d\boldsymbol{l}_\mathrm{p}$$

$$\mathcal{A}_r^{-} = \int_{\alpha_+}^{\alpha_-} (\mathbf{A}+\mathbf{A}_\mathrm{p})\cdot d\boldsymbol{l} - \int_{\alpha_{p+}}^{\alpha_-} (\mathbf{A}+\mathbf{A}_\mathrm{p})\cdot d\boldsymbol{l}_\mathrm{p}$$

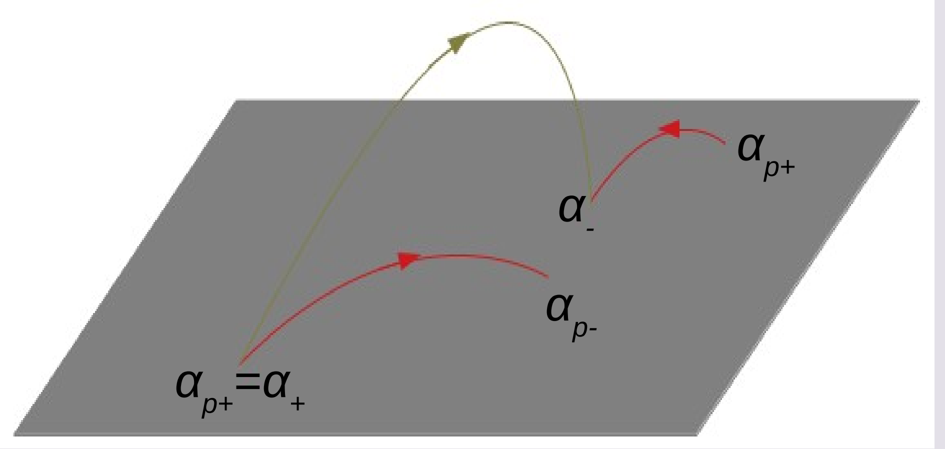

$$\mathcal{A}_r^{0} = \int_{\alpha_+}^{\alpha_-} (\mathbf{A}+\mathbf{A}_\mathrm{p})\cdot d\boldsymbol{l} - \frac{1}{2}\left(\int_{\alpha_+}^{\alpha_{p-}} (\mathbf{A}+\mathbf{A}_\mathrm{p})\cdot d\boldsymbol{l}_\mathrm{p} + \int_{\alpha_{p+}}^{\alpha_-} (\mathbf{A}+\mathbf{A}_\mathrm{p})\cdot d\boldsymbol{l}_\mathrm{p}\right)$$

All are gauge-dependent and in all cases $H_r = \int_{\partial V^s} \mathcal{A}_r^s \, \mathrm{d}\Phi$

Computing RMFLH

Instantaneous finite-volume computation

$$H_r = \int_V (\mathbf{A} + \mathbf{A}_\mathrm{p}) \cdot (\mathbf{B} - \mathbf{B}_\mathrm{p}) \, dV$$

$$\mathcal{A}_r^+ = \int_{\alpha_+}^{\alpha_-} (\mathbf{A} + \mathbf{A}_\mathrm{p}) \cdot dl - \int_{\alpha_+}^{\alpha_{p-}} (\mathbf{A} + \mathbf{A}_\mathrm{p}) \cdot dl_\mathrm{p}$$

$$H_r = \int_{\partial V+} \mathcal{A}_r^+ \, d\Phi$$

1. given $\boldsymbol{B}$ find $\boldsymbol{B}_\mathbf{p}$
2. given $\boldsymbol{B}$, $\boldsymbol{B}_\mathbf{p}$ find $\boldsymbol{A}$, $\boldsymbol{A}_\mathbf{p}$
3. given $\boldsymbol{B}$, $\boldsymbol{B}_\mathbf{p}$ and $\boldsymbol{A}+\boldsymbol{A}_\mathbf{p}$ find RMFLH

Computing RMFLH

Instantaneous finite-volume computation

$$H_r = \int_V (\mathbf{A} + \mathbf{A}_\mathrm{p}) \cdot (\mathbf{B} - \mathbf{B}_\mathrm{p})\, dV$$

$$\mathcal{A}_r^+ = \int_{\alpha_+}^{\alpha_-} (\mathbf{A} + \mathbf{A}_\mathrm{p}) \cdot dl - \int_{\alpha_+}^{\alpha_{p-}} (\mathbf{A} + \mathbf{A}_\mathrm{p}) \cdot dl_\mathrm{p}$$

$$H_r = \int_{\partial V+} \mathcal{A}_r^+ \, d\Phi$$

1. given ***B*** find ***B***$_\mathbf{p}$
2. given ***B***, ***B***$_\mathbf{p}$ find ***A***, ***A***$_\mathbf{p}$
3. given ***B***, ***B***$_\mathbf{p}$ and ***A+A***$_\mathbf{p}$ find RMFLH

Computing RMFLH

Step 3 – Field line integrations

FL integration routine: modification of QSL Squasher code (Tassev & Savcheva 2016) which uses adaptive RK in C++, fast and robust

- same method for both field line integrations
- omit QSL part, keep only FL integration part
- addition of one more equation $$\frac{\mathrm{d}h}{\mathrm{d}s} = \frac{(\mathbf{A} + \mathbf{A}_{\mathrm{p}}) \cdot \mathbf{B}}{B}$$

  to the system
  solved by the code $$\frac{\mathrm{d}\boldsymbol{l}}{\mathrm{d}s} = \frac{\mathbf{B}}{B}$$

- user-supplied starting points instead of automatically determined

Validation with MHD data

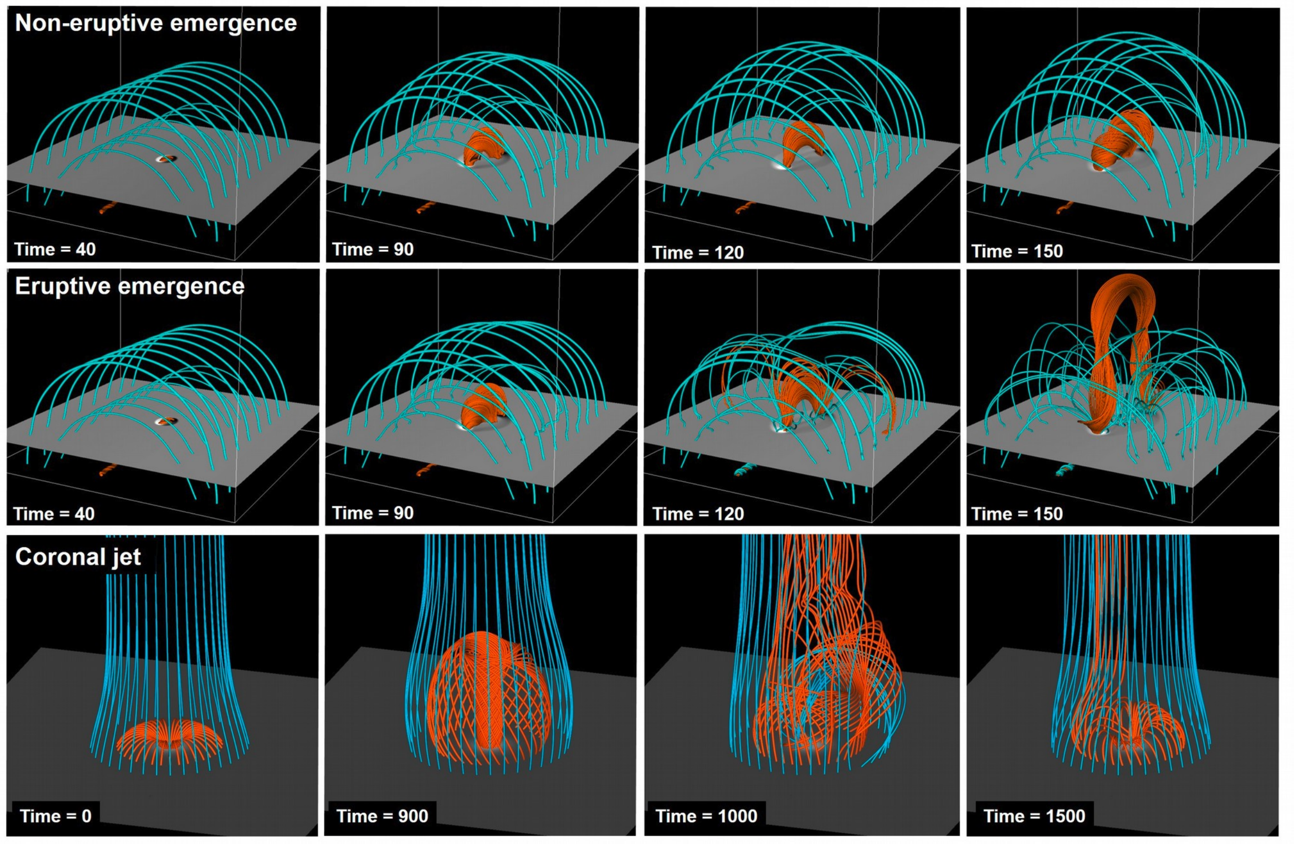

MHD simulations:

Non-eruptive flux emergence
Leake et al. (2013)

Eruptive flux emergence
Leake et al. (2014)

Coronal jet formation
Pariat et al. (2009, 2010)

Validation results

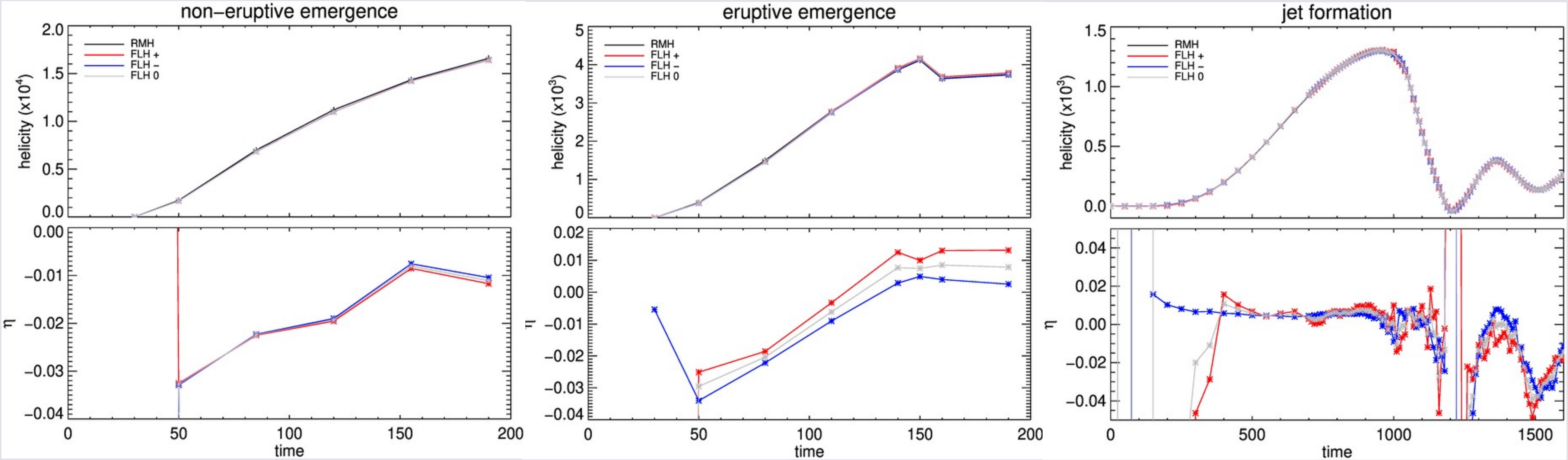

2D visualization of RMFLH

$$\mathcal{A}_r^0 = \int_{\alpha_+}^{\alpha_-} (\mathbf{A}+\mathbf{A}_\mathrm{p})\cdot dl - \frac{1}{2}\left(\int_{\alpha_+}^{\alpha_{p-}} (\mathbf{A}+\mathbf{A}_\mathrm{p})\cdot dl_\mathrm{p} + \int_{\alpha_{p+}}^{\alpha_-} (\mathbf{A}+\mathbf{A}_\mathrm{p})\cdot dl_\mathrm{p}\right)$$

1st term

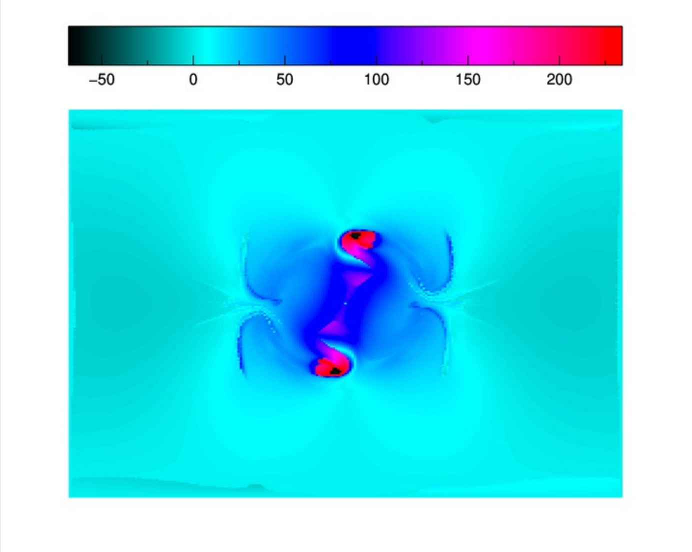

2nd term

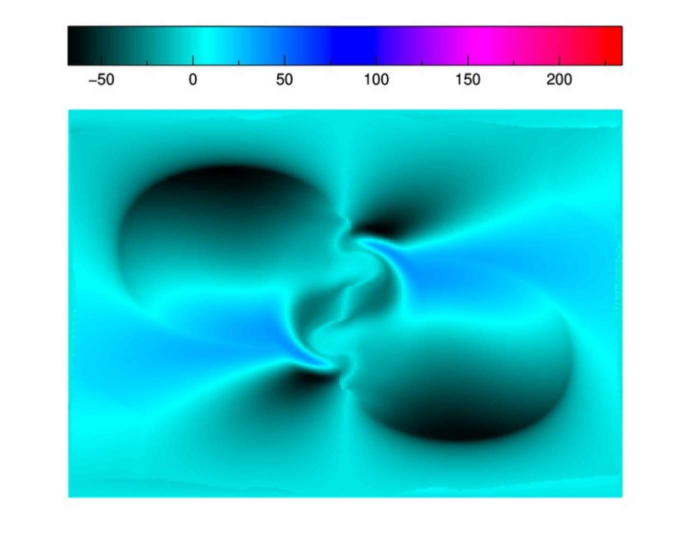

total

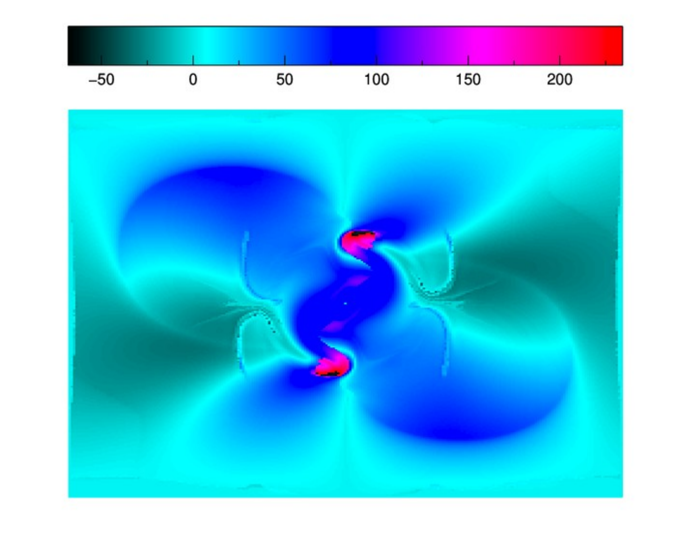

non-eruptive, t=120 @ z=0, FL0
gauge-dependent images

3D visualization of RMFLH

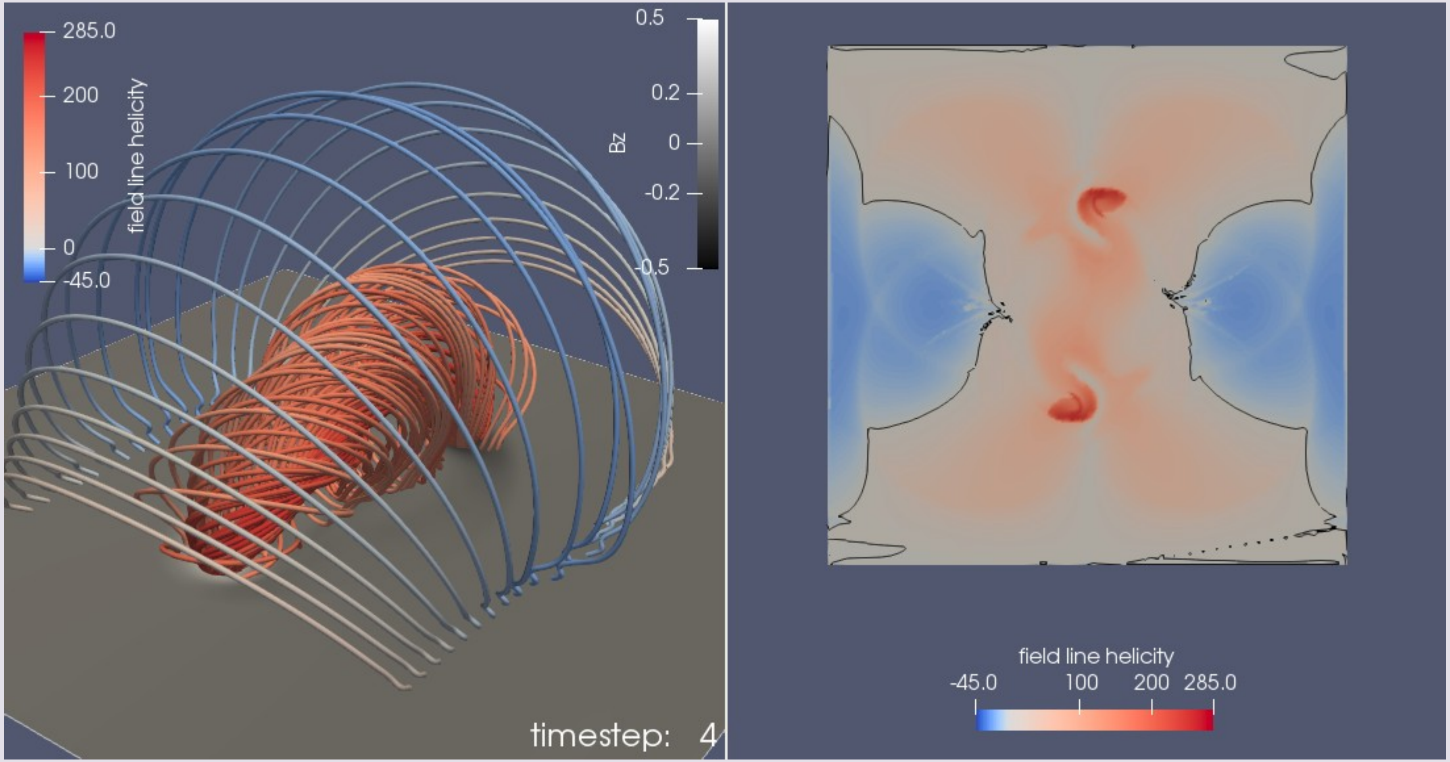

Non-eruptive flux emergence
simulation

3D visualization of RMFLH

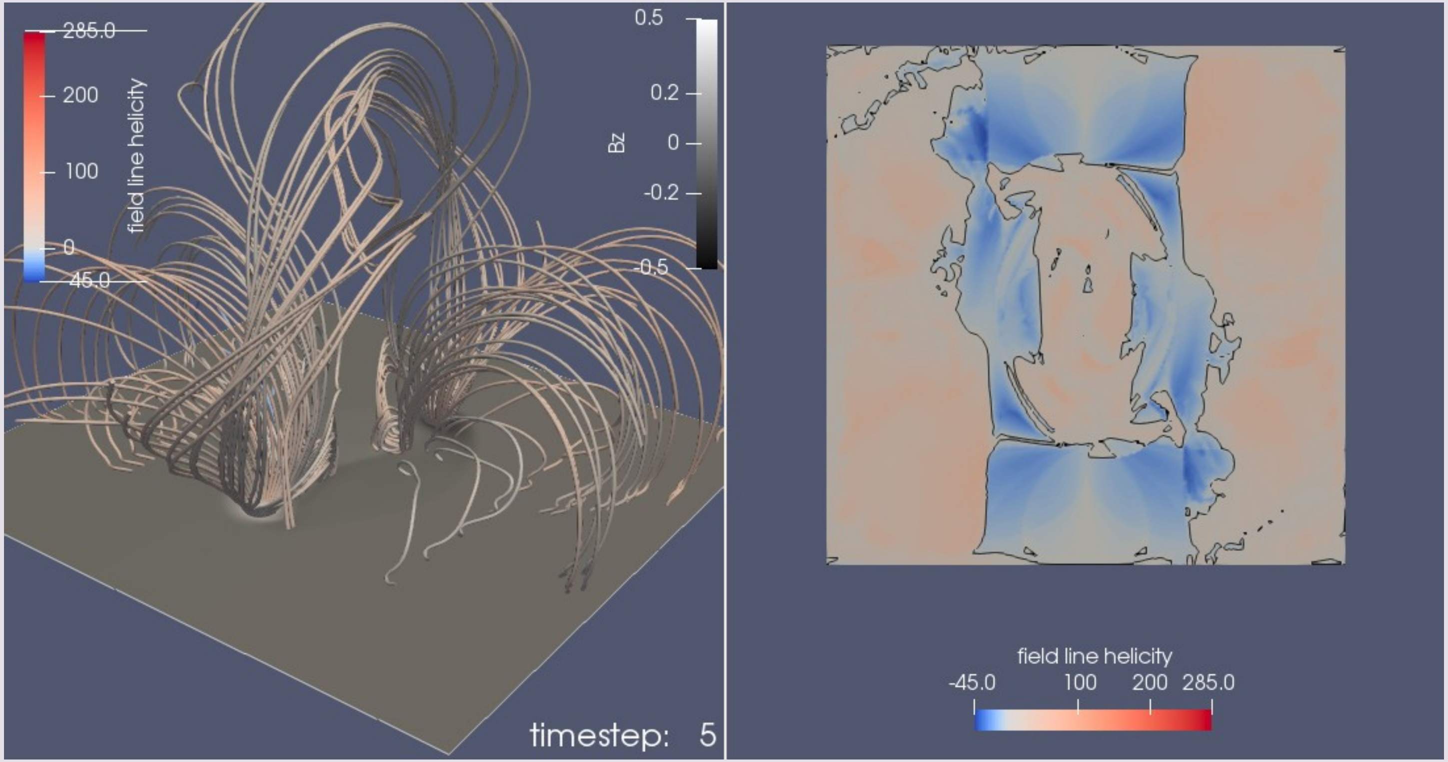

Eruptive flux emergence simulation

3D visualization of RMFLH

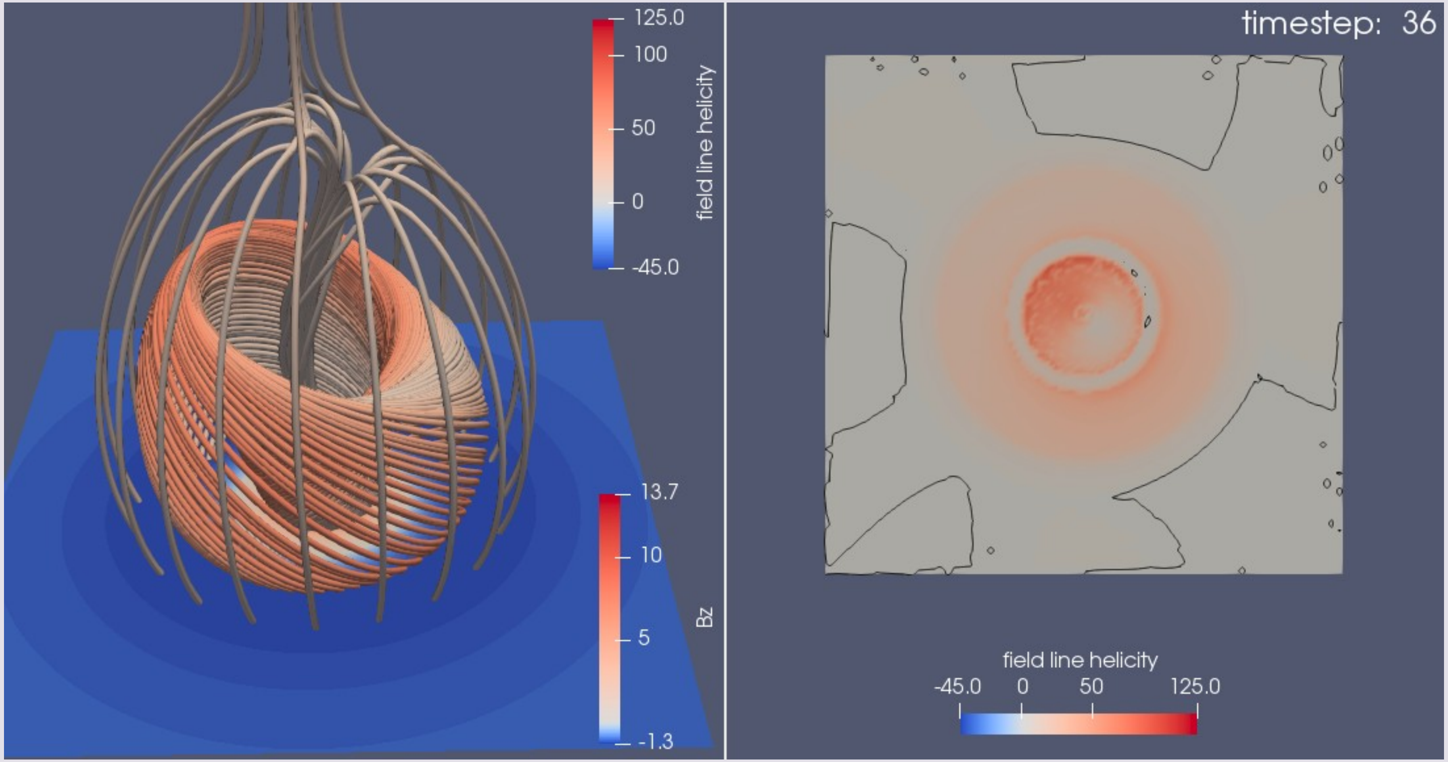

Jet formation simulation

Conclusions

- Magnetic helicity is very important in studies of magnetized systems thanks to a range of useful properties
- The appropriate expression in astrophysical conditions is relative magnetic helicity
- Relative magnetic helicity is hard to compute, and for this, accurate computational methods appeared only recently
- Finite-volume methods provide the most accurate helicity values. Many methods exist in Cartesian coordinates that agree to a high degree
- First development of a computational method in spherical geometry
- Mathematical derivation of proper RMFLH without any gauge restrictions, validation against 3 MHD simulations
- RMFLH has important potential in highlighting locations of intense helicity
- A lot more can be developed/examined